Comparing the effects of winter storms Corrie and Eunice on Noordwijk using laser data

Dalia Madi

Responsible supervisors : R.C. Lindenbergh
Mieke Kuschnerus
Sierd de Vries

Project duration : 16-04-2022 to 16-06-2022

Abstract

As climate forcings due to projected climate change advance, winter storms have been seen to be a nearly annual event in the Netherlands. The year 2022 commenced with the occurrence of storms Corrie and Eunice consecutively, separated by a 16 day period between storms. These storms brought about extreme wind speeds and storm surges thus impacting many urban beaches such as Noordwijk. Many remote sensing tools are enlisted to monitor the coast, of which laser scans are incredibly useful in studying elevation changes. The morphodynamics of the beach and its evolution due to storms can then be studied to obtain a better understanding of the storms. Moreover, storm damage models can be generated, and by understanding the magnitudes of these damages, protective measures can be placed to safeguard against elevated sea level and windspeeds. This research focuses on studying the effects of these storms by means of quantifying the changes. By knowing how much change occured, comparisons of storm impacts can then be made and predictions for future storms are improved.

Contents

1 Introduction

The effects of winter storms, such as storms Corrie and Eunice on Dutch beaches has recently emerged to be an incredibly relevant topic due to the avid effects of climate change. Dutch coasts are continuously threatened by extreme storm events that bring about intense periods of high wave energy and extremely powerful wind gusts. Storm surges lead to major morphological changes along coastlines and dunes , predominantly erosive in nature. The effects of these erosional patterns can be quantified by various remote sensing methods. Of these methods, permanent laser scanners, such as one placed atop of a hotel in Noordwijk, continuously monitors the beach and acquires point clouds at an hourly rate. This powerful tool enables for the determination of elevation values spatially. When done correctly, data alignment and gridding are advantageous methods to organise the data such that it can be processed easily and changes can be quantified. However, simply understanding what happens is insufficient without accounting for the reasoning behind these changes. Only then , conclusions can be drawn regarding the behaviour and response of the beach to extreme, dynamic events such as storms Corrie and Eunice.

This research aims to understand the effects of the above mentioned storms on a beach strip situated in the coastal town of Noordwijk. The determination of the beginning and ending of these storms is initially carried out to extract data sets acquired at an appropriate time to be able to carry out a fair comparative analyses. By studying tidal, wind speed, precipitation intensity time periods, appropriate scans can be chosen for data processing. Multiple existing methods are carried out to detect changes. Of these methods, difference maps, statistical analyses, volumetric changes and areas impacted are enlisted in this study. Moreover, topographic analyses by means of cross sections along chosen transects are used to obtain a better understanding of the evolution of the beach profile due to the storms. This is done not only before and after the storms, but in between them as well. The advantage of doing this is the ability to determine whether the beach experienced recovery between the storms, or if the effects of the storms can be directly superimposed, as erosion is expected between the storms. Finally, this study also attempts to reason these changes, by accounting for the weather conditions, and the impacts of airflow diversion due to the presence of artificial structures on the beach, namely the beachclub at the center of the beach. Other anthropogenic factors are also highlighted in this study, and attempts to differentiate them from naturally occurring features is made.

This research defines sandy beaches and discusses current monitoring methods enlisted in studying the dutch coast in **section 2**. Following this , the study area is described in great detail in **section 3**, as well as the datasets used in the study. These include the weather data, and the laser, including the configuration of the scanner and its properties. The methodology enlisted to detect changes on the beach are then discussed in **section 4**. Lastly, the results are displayed and interpreted in **section 5** and are later reasoned by returning to the weather data. By doing so, changes can be understood and easily interpreted.

1.1 Purpose and objectives

This research is geared towards answering the following research question:

- Which of the two storms, Eunice or Corrie, had a greater impact on the beach in Noordwijk?

To answer this, a few other sub-research questions are answered:

- When did the storms happen and how can weather data be used to determine the start and end of a storm?
- How can changes occurring on the beach profile be quantified?
- Where do the greatest changes occur along the beach and are there reasons for this change?

1.2 Scope of research

To be able to carry out this research, data is acquired before and after every storm. Although compelling, scans acquired during the storm are not used and deemed unfit for the research. This is due to decreased clarity occurring due to poor weather conditions, and elevated rain and fog levels. Moreover, not much information can be derived without studying the situation before and after. The assessment involves looking at changes in elevation, areas impacted, sand volume and topographic changes as well. The research does not dive too deep into the anthropogenic factors, although mentioned, that cause these changes, but is more focused on naturally occurring events and processes.

1.3 Significant assumptions and limitations

To be able to carry out this research, a few assumptions are made, without forgetting that the study also contains major limitations. These assumptions and limitations are are highlighted below:

Assumptions:

- The storms impacted the beach differently due to different weather conditions.
- The storm events are separate events. Storm Dudley also occurs at the end of February and is still regarded as storm Eunice .
- The laser scanner is precise and calibrated correctly, with little errors.

Limitations:

- Anthropogenic processes occur on the beach and must be seperated from natural ones.
- The number of laser points are unequal in the before and after storm datasets; more points are present before the storms. This means that where data is present in one location might not be the case in the other dataset. Point pair comparisons can be nearly impossible as the laser scanner nearly never scans the same point twice.
- Gaps may be present in the data.
- The laser data can not be validated due to the lack of additional data at the exact time frame that the laser scans are acquired in.

1.4 Workflow outline

The following steps were carried out to carry out this study;

1. Study the weather data for tidal , wind, precipitation intensity and wind direction variations.
2. Decide appropriate times of scans for both storms to obtain four datasets; 2 before and 2 after each storm.
3. Read the laser data and align it using internal properties of the scanner.
4. Identify areas of interest and the presence of any disturbances in the data by looking at images acquired from the beach.
5. Generate grids of 1m resolution for the entire beach, ensuring to divide the beach into a north and south section. For smaller areas of interest, resolutions of and 0.5m and 0.25m are enlisted.
6. Quantify changes on the northern and southern parts of the beach by means of difference maps, histograms, areas impacted by accretion and erosion, sand volumetric changes and topographic variations.
7. Analyse and interpret these changes , comparing the impacts of both storms on different locations in the beach.
8. Reason the changes by looking back at weather conditions , aeolian processes and the impacts of artificial structures on sediment transport.

2 Monitoring storm damages on sandy beaches

In recent years, coastal processes have been researched more comprehensively, owing to the advancement in measuring techniques and greater interest to monitor coastal areas due to projected climate change. Increasing storm surges and unpredictable storm patterns threaten over 2.4 billion people, of which most live less than 100km from the coast [8]. These inhabitants are exposed to extreme storm events and are also faced with greater challenges such as coastal inundation and erosion. Changes in the sediment budget of coasts are dominated by strong winds and have been seen to influence the morphology of beaches worldwide. Understanding coastal process has become a key research area in the Netherlands and Belgium, countries also affected by coastal and dune erosion [15].
These dunes, undergoing continuous accretion and erosion, enable a greater understanding of the potential damages of storms on sandy beaches. The quantification of these damages gives information on the magnitude of these storms, the potential hazards the storms bring, and most importantly, enables the creation of storm damage models on the sandy beaches. Remote sensing techniques such as Global Positioning Systems(GPS), terrestrial laser scanners and more recently, drones are commonly used to remotely monitor sandy beaches worldwide. These methods offer a greater understanding of time-varying beach profiles and can be powerful tools to understand beach resilience after hazardous events such as storms.

This chapter aims to define sandy beaches , showcased in **subsection 2.1** and to demonstrate monitoring methods currently enlisted to quantify changes in their sediment budget, described in **subsection 2.2**. Moreover, terrestrial laser scanners are discussed and compared with other methods, with their limitations considered as well.

2.1 Characteristics of Dutch sandy beaches

When understanding how storms impact beaches, it is necessary to develop a deeper understanding of sandy beach morphodynamics, and what they constitute. The 400km Dutch coastline is comprised of expansive sandy beaches, characterised by dune ridges that are oftentimes vegetated. These ridges are composed of fine to medium-sized aeolian (windblown) sands and play a major role in ensuring the protection of the coast against erosional processes and coastal flooding[3]. The shape of the dune fields is often unstable as variations in wave action, wind patterns, sediment supply and geomorphological changes of the beach directly affect their size and morphology[7]. Moreover, beach profiles are also subject to anthropogenic changes, beach nourishment and construction works are frequently occurring along the Dutch coastline.

During a storm, elevated wind speeds and storm surge water levels erode the beach and dunes and alter their morphology. This occurs as sufficient wave energy brings about sediments from the sea bed, and sufficient wind forces pick up fine sand particles and deposit them elsewhere. This leads to continuous erosional and accretional patterns depending on the direction and rate of transport. Figure 1 showcases a typical Dutch beach profile.

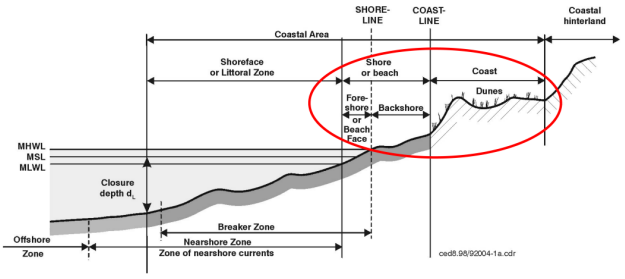

Figure 1: Cross section of a typical Dutch coastline [3]

As shown in Figure 1, the coastal area is characterised by the presence of dunes, a backshore, a beach face and a breaker zone. Sea level however is liable to change during the event of a storm, reaching a storm surge level, a combination of the predictable astronomical tides and the storm surge itself. The beach is made up of unconsolidated sand, along a relatively horizontal surface, typically 250m in width. The back-shore, a subdivision of the beach, is located between the dunes and the beach face. It is usually only impacted during periods of

extreme storms , and therefore usually remains dry. [13]

Small scale features are also present, such as ripples and dune vegetation along Dutch beaches. Rippling formed by the action of waves leads to symmetrical patterns due to the oscillatory nature of waves. When formed by wind processes, however, turbulent air currents cause them to be asymmetric in shape allowing them to be distinguished from wave ripples. Vegetation, such as Marram grass and shrubs are also characteristic of Dutch dunes, stabilising them and hence allowing for dune growth [9].

2.2 Remote sensing techniques

Several data acquisition techniques are currently being used to monitor Dutch beaches remotely. Of these methods, airborne, spaceborne and land methods are most popular. This subsection focuses on these methods and describes their advantages and limitations.

2.2.1 Global Position Systems

Global Positioning Systems (GPS), both static and kinematic, are traditional contact methods which allow for the creation of digital elevation models. These models enable you to study variations in beach profiles from the geospatial data collected. Although the data collected are typically of low spatial and temporal resolution, they can be used to fill in missing data when used as a surplus for other remote sensing methods and validation. Limitations to GPS methods include their impracticality, and added danger when attempting to sample data in remote locations . Moreover, the signals may be affected by multi-path errors and atmospheric conditions[3].

2.2.2 Airborne Laser Scanning(LIDAR)

This airborne laser scanning method relies on the release of laser pulses, which are reflected and detected by a device situated on an aircraft. With the aid of an accurate interval timer, the round trip travel times of the laser pulses from the aircraft to the ground are measured and the time intervals are transformed into range measurements by accounting for the speed of light. Raw ground coordinates are then obtained after the range data is processed [14]. This method can be very useful when dealing with a large study area as an aircraft can cover great distances. [15] . In addition, data acquisition is accurate and rapid and can be used to map inaccessible areas. The dataset, known as Jarkus data, is collected once a year however and therefore large time gaps are present between the consecutive datasets. Moreover, operation costs can be greater and as aircrafts are used , flights must be appropriately scheduled and are difficult to organize. Also, using this method during periods of heavy rain or low hanging clouds gives poor scans due to refraction effects. Figure 2 below depicts the scanning methodology described above.

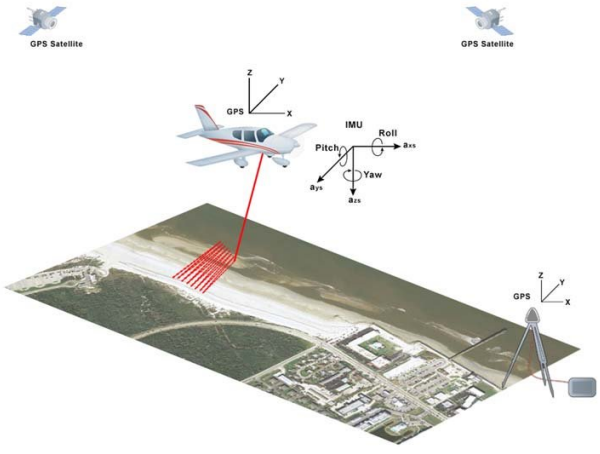

Figure 2: Principles of airborne LIDAR methods [14]

2.2.3 Photogrammetry

This method uses the overlapping of two or more images to obtain geospatial measurements. The underlying principle, known as stereovision, is based on the geometry of perspective scenes [17]. This essentially requires the overlap of 2 or more images to produce a stereoimage which can be later processed. The photographs of the beaches are obtained either aerially or terrestrially, and drones have been recently enlisted too for this purpose. Digital photogrammetry can be used to obtain digital elevation models of the coastline and beach. The images however require position and orientation systems, (POS) which ensure the correct alignment of the images [17]. A drawback of this method however is that it requires good weather and optimum tidal conditions to obtain clear photographs that can be later processed. Photogrammetry can also be quite expensive and image processing can be time-consuming [5]. Figure 3 blow depicts the working principles of photogrammetry.

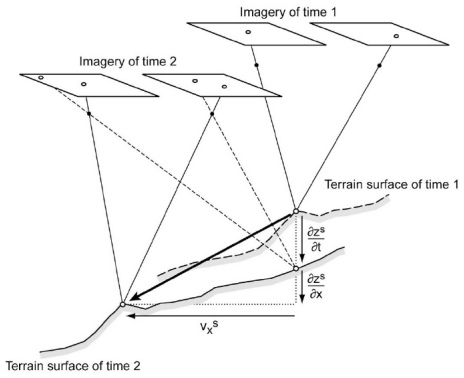

Figure 3: Principles of photogrammetry[12]

2.2.4 Permanent laser scanners

Geomorphological changes in sandy beaches can also be quantified using terrestrial laser scanners (TLS) and permanent laser scanners(PLS). These methods differ as incidental TLS involves frequenting the beach on separate occasions to acquire scans. On the other hand PLS are placed in a location and fixed, continuously generating scans at a programmed interval. These scanners are able to produce high resolution images by means of projecting laser pulses on objects and obtaining millions of datapoints , called pointclouds. These datapoints also contain geospatial information(X, Y, Z coordinates) which can be further processed. This method is known to outperform airborne LIDAR data and is also known to be beneficial when surveying a smaller areas in great detail. Scans can also be generated frequently , thereby offering a higher temporal resolution[16]. Moreover, they are incredibly beneficial in scanning dynamic environments exposed to sudden storms , such as beaches and coastal regions [6]. Information on surface roughness, elevation changes and hence volumetric changes in beaches can also be calculated. Overall PLS is a great way to monitor beaches such as Noordwijk that experience frequently occurring winter storms. As this method has the fewest limitations and greatest accuracy, this research is carried out using PLS data. Figure 4

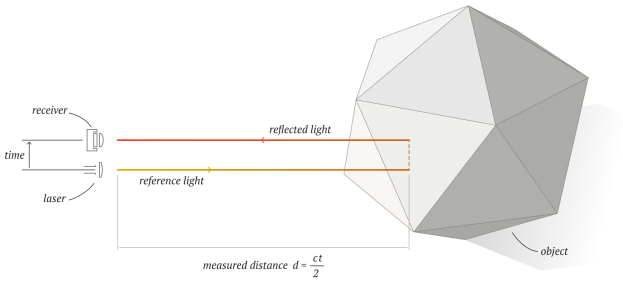

Figure 4: Principles of PLS [4]

3 Data set description and study area

This sections aims to highlight all the key features that the beach constitutes, to give a better understanding of the real life situation at the beach. Firstly, an overview of the beach location in relation to its location in the Netherlands in presented. Following this, a detailed description of the features present in the beach is provided, shown in **subsection 3.1**. This is followed by a preliminary analysis of the weather data in **subsection 3.2**. Lastly, the laser scanner configuration and the point cloud dataset specifications are discussed in **subsection 3.3**.

3.1 Regional Description of study area

3.1.1 General overview of beach location

The study area is situated on the Dutch coast; a popular beach in the area of Noordwijk. The beach, dependant on tidal variations , is approximately 130m in width. This value is known to significantly decrease to 80m during a period of storm surge [1]. The study area is located in front of a Hotel called the " Grand Hotel Huis Ter Duin" , only 150m away from the beach strip. The area is known to be frequented by visitors, and receives a lot of anthropogenic input such as construction, bulldozer works and other touristic activities. In front of the hotel, a row of vegetated sand dunes are present which act as a natural barrier to the inland. The dunes are subjected to yearlong variations but are especially affected by winter storms bringing about large wind speed values. For the purpose of the study, a 200m length section is initially taken to account for the entire beach area. When observing more specific variations, smaller areas are later chosen. Moreover, much of the data is filtered to discard areas including and past the dunes, such that only the beach, alongside its features are accounted for. The location of the study area , as well as an aerial image is shown in Figure 5 below.

Figure 5: Study area : Noordwijk

3.1.2 Features present in the beach relevant to dataset

The study area comprises many interesting features that are relevant to the research. Firstly, the presence of dunes leads to a so-called " shadow effect" (see **subsection 4.1**) by which areas in front of the dune are not in the field of view of the scanner and go undetected by the scanner. In addition, inter-tidal bars are present on the beach located between the mean high water level and mean low water level. These bars are known to migrate during storms as large amounts of sediments stored underwater move towards the beach and accumulate. The shape and morphology of the bars differ laterally as closer to the beach, they appear flatter due to higher wave energies, yet progressively become more chaotic in structure as the wave loses energy more inland. Aside from these natural structures, artificial structures are present such as the beach breaker's cafe, surrounded by containers and equipment. Moreover, a trailer is present 60m north of the cafe. The trailer also leads to a small shadow effect. Adjacent to this trailer, concrete tiles can be found placed in a grid-like formation. These grids are not present in the datasets before the storms but do appear later after storms and are seen to be displaced due to wave action. Lastly, artificial protective embankments for the cafe and markings on the sand such as tyre tracks, bulldozer marks, human and animal footprints are observed in the study area. These features are shown in the Figure 6 below, their relevance summarised in Table 1 below

Figure 6: Features present in the beach data [14]

Table 1: Study area features and their relevance to the study

Feature	Relevance to study
foot prints	present in the main dataset and are later ignored
small trailer	artificial structure observed in difference maps, cause for a shadow effect.
tyre tracks	anthropogenic elevation difference (+/- 5cm)
concrete tiles	appears in difference map displaced after storms
inter-tidal bar	cause for extreme height changes after storm
beach club roof	causes shadow effect in data
embankment	area undergoing positive elevation changes after storms
vegetated dune	shadow effect on data, aeolian deposits

3.2 Extracting moments of interest from weather data

To be able to answer the subresearch question **" When did the storms happen and how can weather data be used to determine the start and end of a storm"**, weather data must be analysed. The weather data was obtained in accordance to the Royal Netherlands Meteorological Institute(KNMI), as well as the Rijkswaterstaat, the general directorate for public works and water management. The former provided data on wind speed, precipitation intensity, whilst the latter was used to obtain data on the astronomical tides. Weather data was used to enable a better selection criterion for the laser scans as high tides are unfavourable due to the presence of water which goes undetected by the laser scanners. The wind speed and precipitation data were collected from the Noordwijkerhout station (52.2541° N, 4.4894° E) , situated roughly 5 kms from the study area. The tidal data studied however was obtained from the IJmuiden buitenhaven (52.4569°N, 4.6060° E), a harbour situated north 23 km from the study area. Although an alternative harbour, Scheveningen (52.1024° N, 4.3022° E) is nearly equidistant to Noordwijk , the latter station was better representative of the tidal situation in Noordwijk. By studying the tidal variation patterns in the Netherlands, 12 hour tide shifts are observed to occur from the south west to the north east of the country, with decreasing shifts in the northerly direction [11]. This was therefore a suitable motivator to accept the IJmuiden data as relevant for the study, as it is located more north.

A crucial step in understanding the effects of the storm is to be able to define its start and end point. As storms are continuous events, it is therefore more favourable to treat their start and end not as exact points, but rather windows of time. For storms Corrie and Eunice, this is evident when plotting the time series of the wind speed and precipitation intensity. A sudden increase in wind speed and precipitation intensity are a good indicator of the start of a storm. The wind speed is first studied for both storms, followed by the

precipitation intensity. It is then realised that during storm Corrie, an upsurge in the wind speed occurring after the 31st of January, brings about wind speeds up to 10 m/s. Prior to this upsurge, a minor upsurge event occurs too before the storm. As the storm comes to its end, wind speeds drop to their regular values of approximately 2 m/s. A similar pattern is observed with storm Eunice, however, the wind speed intensifies around the 21st of February, reaching a maximum value of approximately 8m/s. Note that the weather station chosen is not exactly at the beach therefore wind speeds experienced in the beach are expected to be even higher.

Although wind speed data provides a good understanding on storm development , changes in the precipitation intensity when studied simultaneously with the wind speed data can be advantageous in better understanding the behaviour of the extra-tropical storms Eunice and Corrie. The precipitation intensity was studied and a maximum precipitation intensity of 8mm/hr is seen to occur during storm Corrie. This value is slightly greater for storm Eunice, a peak of 14 mm/hr of precipitation occurring on the 18th of February.The combined time series were then studied for both storms, with the tide data. Times of extreme low tides were used to identify possible suitable time options for the laser data. This was used as a primary criterion, followed by placing wind speed and precipitation intensity thresholds of 4m/s, and 0 mm/hr respectively. The wind speed threshold was defined by recognising atypical wind speed values than those regularly experienced for the study area. The precipitation intensity criterion however was given greater importance, as the lack of precipitation leads to clear scans, with a greater field of view and less "no-reflection" data present in the point cloud [10]. Consequently, this then facilitates data processing and interpretation of the laser points in the point cloud. The combined time series are displayed in the Figure 7. This then yields four data sets ; 2 from before the storms and 2 from after.

The chosen times of scan of the data sets are shown in the figure are summarised in Table 2

Table 2: Chosen dates and times of acquired scans

Storm name	**Before Date & time**	**After Date & time**
Corrie	29/01/2022 08:00	02/02/2022 03:00
Eunice	16/02/2022 12:00	21/02/2022 15:59

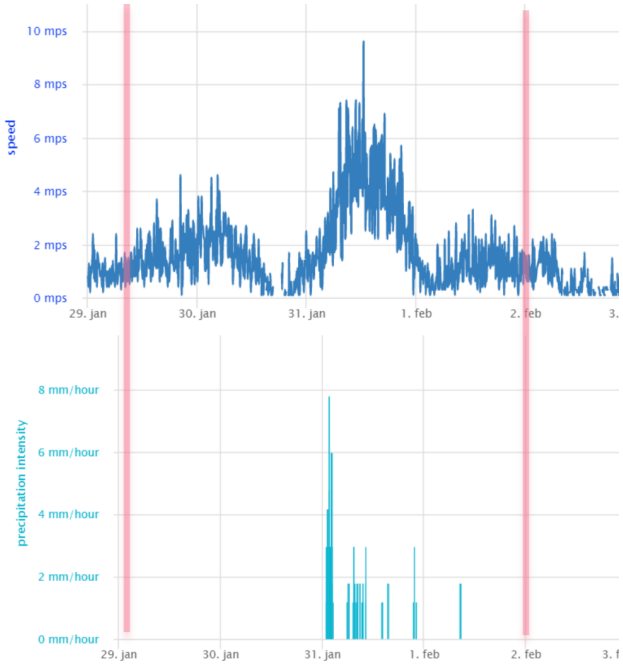

(a) Storm Corrie

(b) Storm Eunice

Figure 7: Combined time series of wind speed and precipitation intensities for storms Corrie and Eunice. The figures contain red stripes on the time series, indicative of the date and time chosen as a suitable "before" and "after" time frame for the laser datasets respectively.

3.3 Point cloud data set specifications and scanning configuration

The point clouds were acquired using the Riegl VZ-2000 Terrestrial laser scanner(TLS). The scanner, situated atop a hotel overlooking the beach, Grand Hotel Huis Ter Duin, continually scans the beach and neighbouring dunes at an hourly scanning rate. The scanner , shown in Figure 8, is highly accurate, and enables for simultaneous

image and scan data acquisition. The specifications of the scanner are highlighted and described in detail in Table 3 below . It is crucial to note that incidence angle and point spacing varies in the dataset and the values listed are merely estimated, and averaged values.

Figure 8: The Riegl VZ-2000 scanner

Table 3: Laser scanner specifications of the Riegl VZ-2000. Note that the incidence angle and point spacing are approximations and not exact values. [2]

Property	**Value**	**Unit**
Angular Resolution	0.03	° deg
Wavelength	1550	nm
Incidence angle	∼77	° deg
Beam divergence	0.27	mrad
Point spacing	∼10	cm
Scanner height above sea level	55	m

The four data sets obtained contain millions of point clouds, and are placed into a .laz format. In addition to this, an alignment file is provided to rotate the data for inclination changes. Under normal circumstances, this is not necessary for a short period time, as it can be assumed that the scanner remains fixed in position. However, as we are dealing with storm events, this must be accounted for due to possible sudden movements of the scanner caused by elevated wind speeds. The reference datum is taken to be the top of the hotel, the location of the scanner. As the scanner scans downwards, elevations detected are outputted as negative values.
The data sets initially contain scanned points, inclusive of the dunes and the beach house. As the angular resolution is 0.03°, the scans are considered to be of lower resolution. Moreover, outliers are initially present, and values exceeding the beach domain are noticed. Scanned points exceeding the elevation of the hotel are accounted for, with possibilities of birds being scanned too. The point clouds consist of regions with missing data that need to be accounted for, occurring in areas that are outside the field of view of the scanner ; behind the dunes, and the beach club. The interface between the sea and the start of the beach mark a boundary between the presence and absence of points. Although the average point spacing is 10cm, this value increases significantly at much larger ranges (>200m). On the other hand, in areas quite close to the scanner such as the beach club roof, this value is seen to be much smaller, approximately 5 cm.

4 Change detection methodology

This chapter focuses on answering the subresearch question **" How can changes occuring on the beach profile be quantified "**. This is done by looking at various change detection methodologies to quantify the storm-induced changes. Importing and alignment is initially introduced in **subsection 4.1** and **subsection 4.2** , followed by the grid creation process in **subsection 4.3**. Elevation difference maps are then generated in **subsection 4.4** and statistical methods used to study them are discussed in **subsection 4.5**. Lastly, areas impacted, volumetric changes in sand and beach profile variations are mentioned in **subsection 4.6**, **subsection 4.7** , **subsection 4.8** respectively.

4.1 Importing and reading the laser data

In order to import the data, it is realised that the file type provided is specifically tailored for laser data. Multiple applications are present and can be used to do so, one of which is called CloudCompare. This is a 3D point cloud processing software, a powerful tool that is useful in dataset visualisation and simple data processing. For this research however, the programming tool Python is enlisted to carry out calculations and to generate plots. The data is initially read into Python, and then filtered. The filtering is done to remove points in the air, on the building, and other points outside the extent of the study area. The initial datum of the acquired scans is the hotel balcony, the location of the scanner. The scanner , however, is situated at an elevation of 55.75 m above the ground. Due to this, the initial elevation values are negative values as the field of view of the scanner is downwards. The datum was then altered to be the ground in order to better perceive the elevation values. Further filtering is then carried out to remove points including, and past the start of the dunes, leaving behind only the beach strip for analysis. Figure 9 below is an example of an imported dataset.

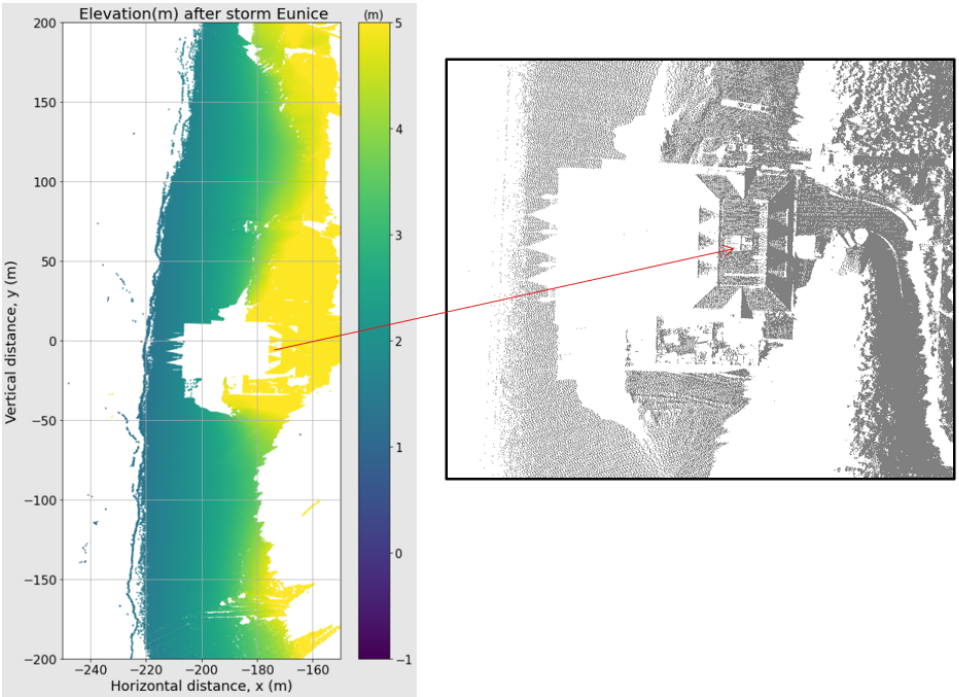

Figure 9: An example of a plotted laser data (using python) highlighting beach elevation variation along the beach strip. The figure to the right indicates the location of the beachclub, a cause for a shadow effect. This is seen as a large white region with no data. This figure is visualised using the CloudCompare software.

As previously described, data gaps are present due to shadow effects. This is seen infront of the beach club , at the center of the figure above. These shadows are also present in the south of the beach, however due to the dunes.

4.2 Dataset Alignment techniques

The datasets are initially misaligned. Multiple factors such as sudden wind-induced movements lead to minor variations in the position of the scanner. To improve the accuracy in the data, alignment must be carried out.

Multiple alignment methods can be utlised to ensure for a more accurate and comparable dataset. An example of this is choosing the same reference point in the datasets, such as a nearby helipad or a flagpost along the beach. For this research however, internal alignment is carried out by applying a rotation matrix on properties of the laser scanner known as roll and pitch. The former's rotational axis is along the longitudinal direction (perpendicular to beach) whilst for the latter, the axis is along the transverse direction (along the beach). By doing so, corrections can be made and more accurate spatial anlyses can be performed. This essentially means that if data is correctly aligned , it can be understood that at a known location a structure is present and not a sand dune for example.

4.3 Comparing the storm datasets by means of grid creation

To be able to compare different datasets, it is common to process the data such that differences can be taken for any coordinate within the dataset. When dealing with individual points, this is not possible as many gaps are present due to the discrete nature of the laser points. Moreover, for any particularly scan, the laser scanner almost never scans the exact point again. The latter can be disadvantageous as no direct comparison can be made for 2 points as they are nearly never in the same position. To solve this issue, geospatial interpolation methods such as Triangulated Irregular Network(TIN), and Kriging can be used to obtain a more continuous dataset. These methods however have their limitations and are oftentimes computationally heavy. Limitations of using TIN include the discontinuous slopes of the triangle edges and sample data points, whilst Kriging requires a trend-less dataset.

A much simpler alternative would be allocating a median value to a pixel after rasterising (gridding) the dataset, such that a grid is created of a known resolution. By doing so, all data points falling under a particular pixel location are evaluated, and their median is taken to eliminate outliers. This results in a single pixel of one elevation value. This process is then repeated for every pixel for the entire dataset. The chosen resolution for the whole beach data set is 1m, yet higher resolutions are later used when quantifying changes in specific areas of interest. After having done this, 2 grids can be easily compared for the same pixel location, and their differences can be taken. This method allows for the quantification and classification of areas experiencing certain elevation difference values. Moreover, volumetric estimations can be done as the area of every individual pixel is known as well as the corresponding elevation difference value.

4.4 Generation of difference maps

Elevation differences are used to compare beach data before and after the storm. Identical pixel locations can be easily identified using the gridded data, and elevation differences can be derived by simply subtracting the initial elevation value from the before storm data set from the final elevation value obtained from the dataset after the storm. Following this, difference maps for the entire beach are generated. This is done for both storms, north and south of the beach. To account for the presence of the beach club in the center of the beach, the beach is divided into north and south locations. As a result, different wave and aeolian depositional and erosional patterns may emerge. The difference maps discussed in this chapter correspond to a grid with a resolution of 1m, but higher resolutions were later generated for specific areas of interest. This was done primarily because increasing the grid resolution for the entire beach was computationally demanding. Furthermore, it would be more interesting to test the grids' sensitivity to higher resolutions when looking at specific areas of interest and calculating volumetric changes. The underlying equation used in the difference map generation is shown in Equation 1 below.

$$\Delta Z_i = Z_{i+1} - Z_i \tag{1}$$

- ΔZ_i : Elevation difference in m at known pixel location
- Z_{i+1} : Elevation after storm in m
- Z_i : Elevation before storm in m
- i : Known pixel location

4.5 Elevation difference comparisons using statistical methods

To compare the datasets, a preliminary study of storm-induced elevation differences was performed using histogram generation. This was done for both storms and the beach's north and south locations. As a result, four distinct histograms are obtained. The histogram distributions allow for the identification of changes, as well as their intensity

and spatial distribution. Not only is the elevation difference determined, but the frequency of different elevation differences can also be obtained. Probability distributions for a normal distribution can be obtained by knowing the frequency and count of occurrences. In theory, this is ideal; however, due to the dynamic and unpredictable nature of storms on beaches, the data provided is not symmetric. As a result, determining the likelihood of occurrence of a specific elevation change is difficult. Other properties of the data, however, can be determined, providing ample information on the nature of the dataset. Histograms are used to obtain the following data:

- Mean of dataset
- Standard deviation of dataset
- Skewness of datasets
- Type of distrubtion (unimodal, bimodal, multimodal)

The mean of the dataset is calculated using Equation 2 :

$$\bar{z} = \frac{1}{N}\sum_{i=1}^{N} z_i \tag{2}$$

Where :

- N : Number of observations
- $\bar{z}$: Mean elevation difference
- z_i : Observed elevation difference

The standard deviation is attained by means of Equation 3:

$$s = \sqrt{\frac{1}{N-1}\sum_{i=1}^{N}(z_i - \bar{z})^2} \tag{3}$$

Where :

- s : Standard Deviation
- N : Number of observations
- $\bar{z}$: Mean elevation difference
- z_i : Observed elevation difference

The skewness of the dataset is understood as follows:

1. Positive skew : Mean > Median > Mode
2. No skew : Median = Mode = Mean
3. Negative skew : Mode > Median > Mean

Analyzing the properties mentioned above allows for a preliminary analysis of the beach. The mean provides information on the expected elevation difference, allowing one to estimate how much accretion or erosion occurred. The standard deviation, on the other hand, indicates how evenly distributed the values are. This could show if the beach has a wide range of elevation difference, or if there is a dominant value that appears to be occurring throughout the beach. The skewness of the data can then be investigated to determine the type of distributions that are occurring and whether the expected elevation difference is greater or smaller than the most frequently occurring elevation difference value.

4.6 Quantifying changes by means of areas impacted

The next approach is to observe changes in the beach profile according to areas affected by certain elevation differences. To implement this, the data was filtered following the two thresholds listed below:

1. Threshold 1 : area affected by an elevation difference of 0 to +0.75 m (accretion)
2. Threshold 2 : area affected by an elevation difference of -0.75 to 0 m (erosion)

After analyzing the histograms, it was discovered that these intervals were less sensitive to outliers. The erosional threshold was chosen more arbitrarily because nearly 75 percent of the data fell within this interval. The accretional threshold, on the other hand, was more sensitive. To investigate this, an upper bound of +0.75 and a lower bound of +0.3 were initially chosen. When this was done, only 0.006 percent of the dataset for storm Corrie fell into this interval, whereas this value was 0.01 percent for storm Eunice. Because these values were too small, comparisons would be insignificant, rendering the interval useless. Conversely, if the upperbound was too large, this would then include pixels that have underwent a misalignment. It was therefore crucial to try and avoid including outlier data.

To compute the areas falling within these intervals, the data was filtered for the aforementioned elevation intervals, and the number of pixels remaining in the filtered dataset was counted. This means that for a $1m^2$ resolution grid, the total number of pixels counted represents the total area within the interval, with values displayed in m^2. This procedure was carried out for both storm datasets north and south of the beach. Following the processing, plots are generated. This was first done to calculate the total area covering the accretional threshold; up to 0.75 m elevation increase. This was then repeated to calculate the total area covering the erosional threshold; an elevation decrease up to 0.75m. Equation 4 is used to determine the area affected by each threshold.

$$\Sigma A = \gamma \cdot \gamma \cdot \Sigma P_i \tag{4}$$

Where :

- ΣA : Total affected area in m^2
- γ : resolution in m
- ΣP_i : Total number of pixels falling within the threshold

4.7 Quantification of differences of identical points through volume estimations

Previously, when quantifying the impacts of a storm, a one-dimensional and two-dimensional analysis was performed by computing variations in elevation and areas affected by both storms. However, one limitation is that it is not entirely representative of the beach, and only a small portion is understood by the first and second dimensions. Furthermore, a more global approach was taken by simply measuring changes across the entire beach. Volumetric estimations can be performed by studying three-dimensional changes in order to detect significant changes along the beach profile. A way to do this is to treat every pixel in the grid as a rectangular volume. The base of this rectangle being the area of a pixel in the grid, in m^2. The height of the rectangular volume , however, is changing along the grid. The datum taken would be an elevation difference of 0m. By doing so, the volumes in the positive and negative domain can be summed to obtain an overall volumetric change. A sensitivity analysis can then be done by increasing the resolution of the grid, to obtain more rectangular volumes and potentially more accurate results. As the beach area is quite large and includes areas of anthropogenic input and buildings, specific locations of $900m^2$ area are chosen. These are areas where mainly natural changes are observed to be able to answer the research question fairly. These areas are indicated in Figure 10. Volumetric estimations are carried out for resolutions of 1m, 0.5m, 0.25m. To summarise this, the chosen locations and their extents are shown in Table 4 below:

Table 4: Summary of volume estimation locations

Estimation location	X range	Y range
A	-200m to -170m	+30m to +60m
B	-210m to -180m	+70m to +100m
C	-210m to -180m	-50m to -80m

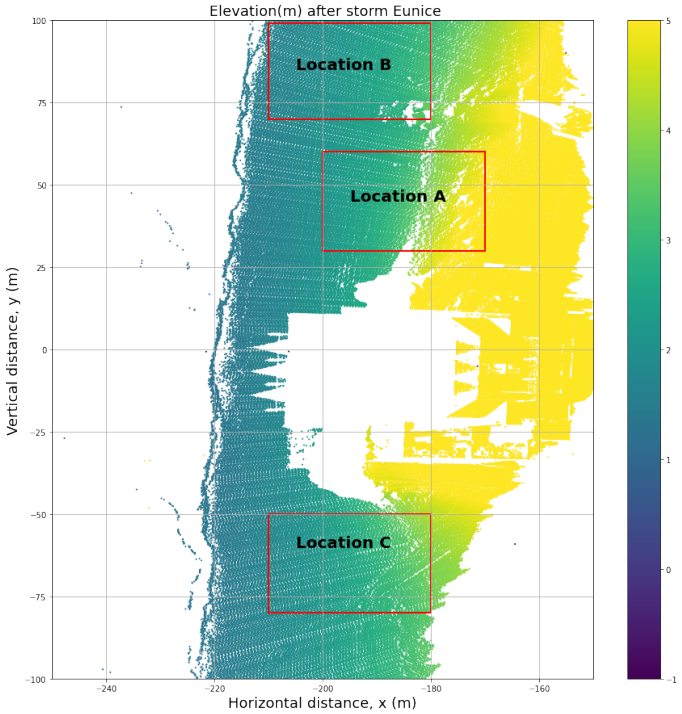

Figure 10: Chosen locations for volumetric estimations.

To calculate the volumetric changes, Equation 5 is enlisted.

$$\Sigma\Delta V = \Sigma\gamma \cdot \gamma \cdot \Delta z_i \tag{5}$$

Where :

- $\Sigma\Delta V$: Total Volumetric change in m^3
- γ : Resolution in m
- Δz_i : Elevation difference in m at a given pixel

4.8 Analysing storm-induced beach profile variations

Another means to study variations along the beach due to the storms involves observing changes in the topography of the beach profile. This can be done by searching for changes along transects at known locations. This is done for both the north and south of the beach. The chosen locations of a north and south transect are indicated in Figure 11 below, their extents mentioned in Table 5. This is carried out by filtering and grouping the dataset to only include data in the specific vertical distance (y) location and generating plots of elevations for both storms, before and after.

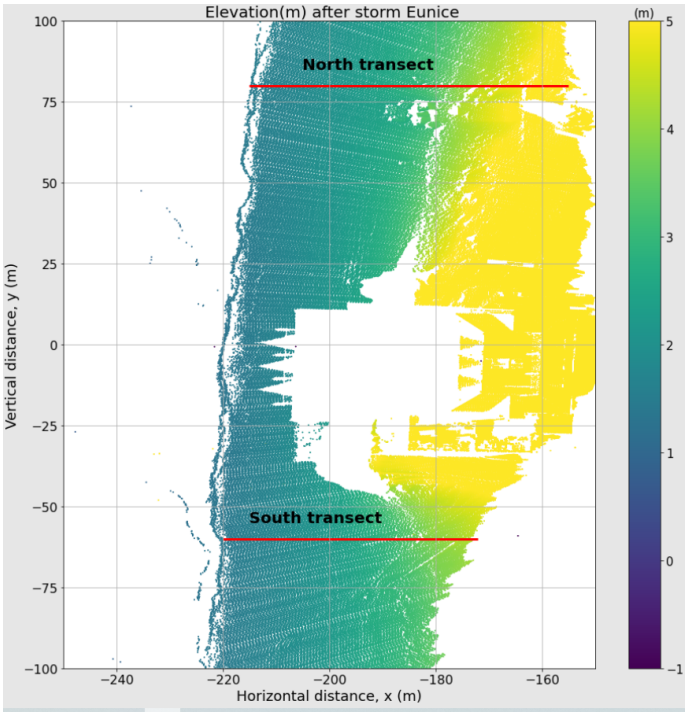

Figure 11: Chosen locations of transects for the cross sectional analysis.

To be able to obtain fair results, multiple transects are generated and no major variations are observed. Therefore the north and south transects chosen are sufficient. Of all change detection methodologies, this step enables for the easiest identification of change as a cross sectional view is easiest to interpret. Overall variations in the beach profile are studied as well as changes that occurred between the storms. This is done as the storm period extended over 25 days and much erosion was expected. By means of a beach profile, the reaction of the beach to extremely energetic and dynamic events such as storms can be studied. A topographic analysis provides plenty of information on beach resilience and any indications of beach recovery.

Table 5: Summary of transect locations

Transect location	**X range**	**Y location**
North	-220m to -160m	+80m
South	-220m to -180m	-60m

5 Results

This section highlights the results of the data processed in the previous section. The section begins with the presentation of the elevation differences before and after storms, as well as histograms displaying the distribution of these differences in **subsection 5.1** and **subsection 5.2** respectively. This is followed by a quantification of areas impacted by an elevation increase and decrease of 0.75m, as well as volumetric changes of sand in **subsection 5.3** and **subsection 5.4** . Lastly, a beach profile analysis , impact summary and overall interpretation is presented in **subsection 5.5** and **subsection 5.6** and **subsection 5.7** respectively.

5.1 Elevation Difference maps : Corrie, Eunice and combined effects

The elevation difference maps are displayed in Figure 12 below for both storms and north and south beach locations. Moreover, a combined difference map is generated showing the overall differences in elevation prior to storm Corrie , to after the occurrence of storm Eunice.

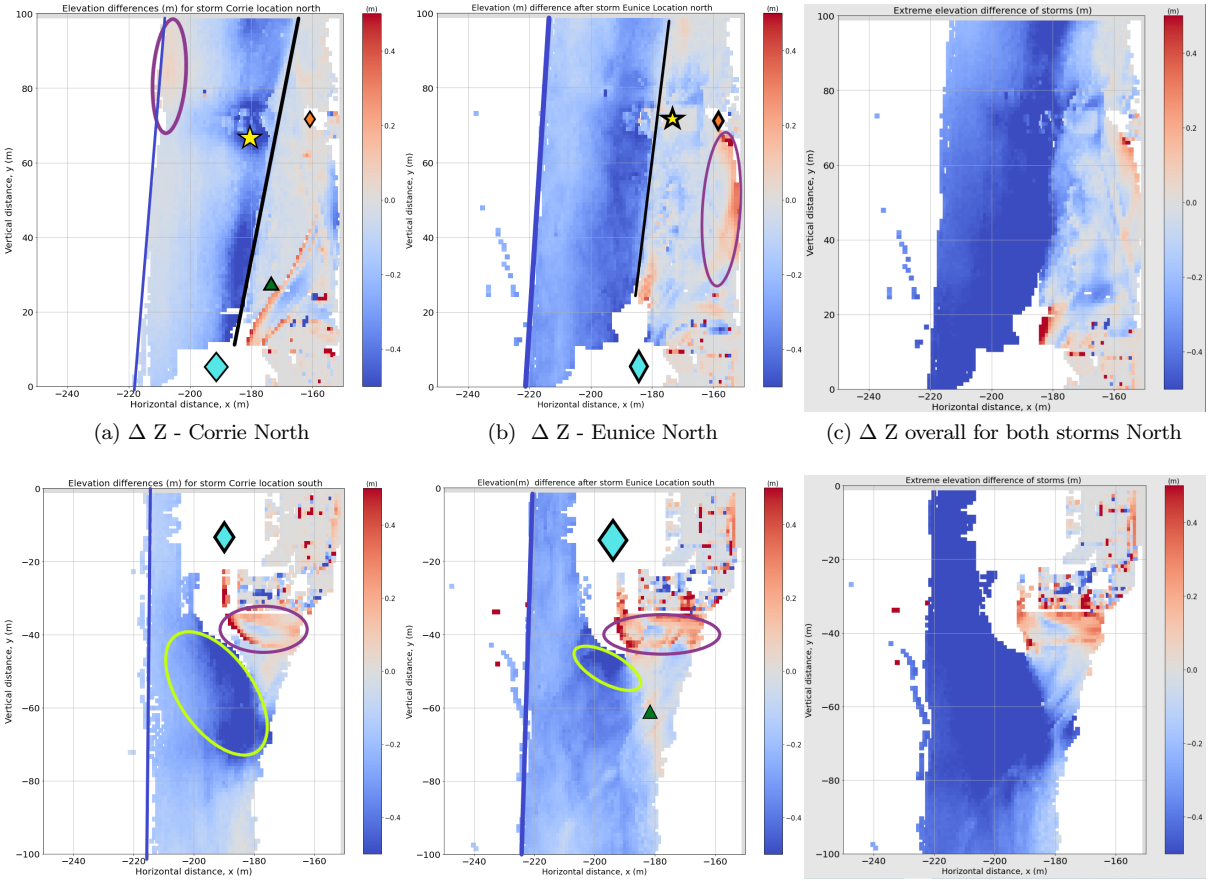

(a) Δ Z - Corrie North (b) Δ Z - Eunice North (c) Δ Z overall for both storms North

(d) Δ Z - Corrie South (e) Δ Z - Eunice South (f) Δ Z overall for both storms South

Figure 12: Elevation differences along the beach profile for north and south of the beach. The location of concrete tiles are indicated by a yellow star, accreted regions are highlighted by a purple circle. The location of the tyre tracks are indicated by a green triangle, the shadow effects by a diamond. The shadow effect caused by the beach club is blue in color, orange due to the trailer. The location of the waterline indicated by a blue line, and a black line at the interface between erosion and lower elevation changes. Lastly, a yellow circle is used to highlight regions with maximum negative elevation changes.

By observing the above figures , it can be seen that the storms resulted in major variations observed in the north and south of the beach. A progressive decrease in beach elevation occurs at increasing horizontal distance from the waterline. In Figure 12a/b, much of the erosion occurs up to the position of the black line, to the right of the waterline. In this region, an overall elevation decrease is observed to occur for both storms. For storm Corrie, this elevation decrease is in the order of magnitude of approximately 0.15 m ,

determined by visually inspecting the figures. However nearby the concrete tiles, a maximum elevation decrease of 0.5m is observed. For storm Eunice however, the maximum elevation decrease is observed to be 0.45m and occurs in 20m wide region, located directly left of the black line. This sand strip is found to begin further up north and to the start of the no-data shadow caused by the beach club in Figure 12a/b, indicated by a blue diamond. In the north, areas located right of the black lines (Figure 14a/b) have experienced minimal elevation height decreases. In other words, these areas have either undergone no elevation change or a slight elevation increase. This is depicted in Figure 12b, highlighted using the purple circle. In this location, an increase in elevation of up to 0.4m is seen to occur due to storm Eunice. For storm Corrie however, the region of maximum elevation increase occurs where tyre tracks are observed in the point clouds. This is indicated by the green triangle in Figure 12a. In this location, an elevation increase of approximately 0.2m occurs, however a 0.2m depression is noticed as well between the accretion lines. Moreover, some accretion is also observed in smaller order of magnitudes of 0.1m, indicated in Figure 12a by a purple circle.

In the south of the beach, the occurrence of the waterline (shown as a blue line), also indicates where elevation decrease commences along the beach. The lack of data caused by the shadow effect on the beach club (blue diamond in Figure 12d, gives little information on elevation changes in that region. A negative elevation difference (erosion) is observed to be widespread in the south , more dominant in areas bounded by the yellow circle in the figures (Figure 12d/e). As seen in Figure 12d, a large area is observed to 0.4m of a negative elevation change due to storm Corrie. For storm Eunice, a smaller area is observed experiencing the same elevation decrease of 0.4m. In Figures 12c/d , it can also be seen that accretion occurs, indicated by the purple circles. A positive elevation change, hence accretion is occurring here due to both storms, yet greater values of positive elevation change are observed to occur due to storm Eunice. Moreover, some accretion is also present in the south , at the location of tyre tracks. This is represented by the green triangle in Figure 12e.

After studying the resultant change in elevation due to both storms , it can be seen that much of the erosion occurring in the north occurs up to the same position of the black lines presented in Figure 12a/b. Moreover, a positive elevation change occurs in the same position as indicated in Figure 12b. Although a positive elevation change too, the magnitude of the elevation change is smaller due to both storms (approximately 0.1m) . Similarly, where accretion occurs in the north due to storm Corrie (indicated by purple circle), an overall elevation decrease occurs for the same position due to both storms. In the south however, a negative elevation difference is prominent. The region of greatest elevation decrease is situated in the location where the yellow circles in Figure 12d/e overlap. As these are overall regions of greatest negative elevation change for both storms. The previously mentioned concrete tiles, trailer and shadow effect are still present overall.

5.2 Histograms of elevation changes

Histograms of elevation changes are displayed in Figure 13 below. This is done for both storms and both north and south of the beach. In the figures, a large peak consistently occurs at an elevation difference of 0m, depicted by the red arrows in the figures. This occurs due to the presence of many pixels in locations of the beach club which did not experience any elevation change as this is an artificial structure. The consistent presence of this peak indicates the correct alignment of datasets as they are comparable.

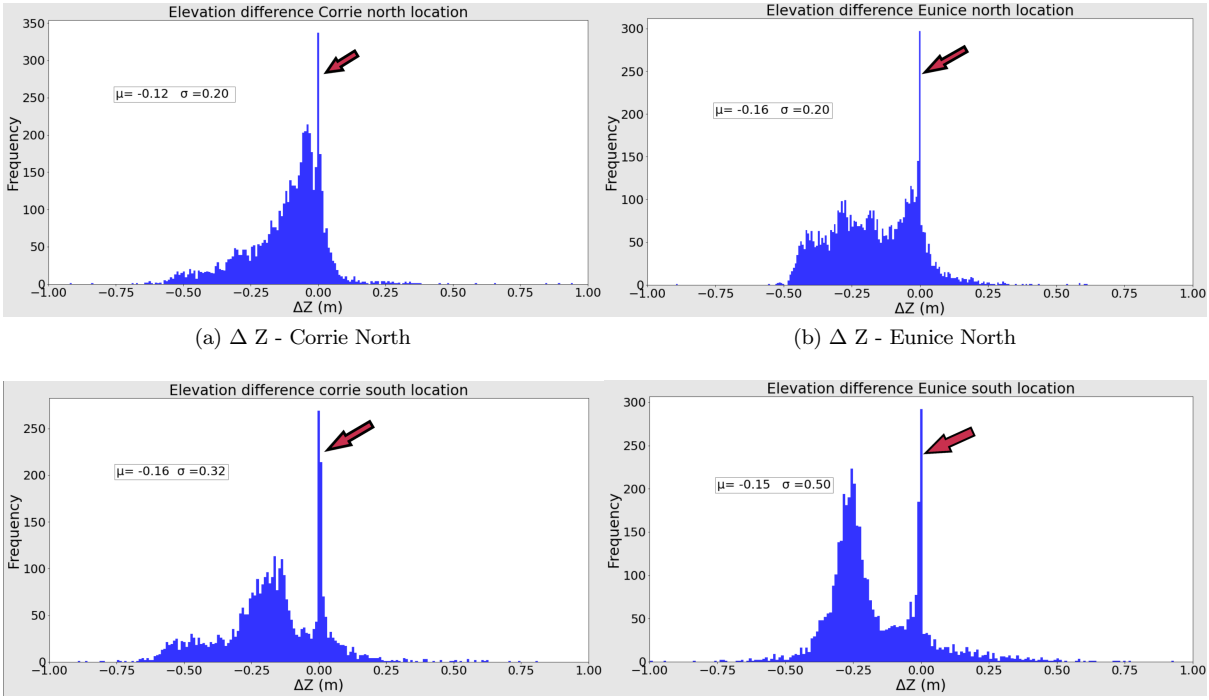

(a) Δ Z - Corrie North

(b) Δ Z - Eunice North

(c) Δ Z - Corrie South

(d) Δ Z - Eunice South

Figure 13: Elevation difference distribution along north and south of beach for both storms

The different distributions show large differences occurring for different storms, and locations too. The skewness and modality varies in the data as seen in Figure 13 above. In Figure 13a , a uni-modal distribution is observed as the data consists of one peak. The data is also negatively skewed as the median is greater than the mean, however, only by a small value of 0.33 cm. In Figure 13b, for the north of the beach impacted by storm Eunice , the elevation differences show a multi-modal distribution. The data is positively skewed as well due to the mean being greater in value than the median. In Figure 13c, the mean and median are approximately equal in value , hence an unskewed dataset is seen. The elevation difference distribution at the south of the beach varies significantly from the north however and the data appears multi-modal. In Figure 13d, it can be seen that the data is bimodal, with a positive skew observed.

In the north of the beach, it can be observed that there is a nearly equal spread in the expected elevation difference values. The height differences in the profiles range from +0.3m to -0.6m for both storms, with the exception of a few outliers. What is different however is that for storm Corrie, the histogram (Figure 13a) displays a large count of elevation differences occurring at only small order of magnitudes of -0.05 to -0.1m. Therefore, a large portion of the northern area experiences smaller order of magnitude elevation decrease. On the other hand , due to storm Eunice, there is no particularly common value of elevation difference expected as elevation differences of different magnitudes are determined for the entire northern area of the beach. To simplify, this means that due to storm Corrie, most of the northern part of beach had eroded by 10cm yet due to Eunice, only a small area experiences the same value of elevation decrease.

Along the south of the beach however, nearly the opposite is observed. Disregarding the peaks occurring at 0m due to the presence of structures, a smaller frequency count occurs for an elevation decrease of 0.25m due to storm Corrie, however a negative elevation change occurs for at different magnitudes ,and no value seems to be most significant. Contrary to this, for storm Eunice, a larger frequency count of up to 0.25m elevation decrease is observed at the south of the beach, but for different magnitudes of elevation loss.

5.3 Quantification of areas affected

The areas affected by an positive elevation change (accretion) up to 0.75m are displayed in Table 6 below.

Table 6: Areas fulfilling threshold 1 ; accretional threshold

Storm name	North area affected (m^2)	South area affected (m^2)	Total area affected (m^2)
Corrie	826	698	1524
Eunice	682	532	1214

To represent this, Figure 14 below indicates the regions where accretion up to 0.75m occurs.

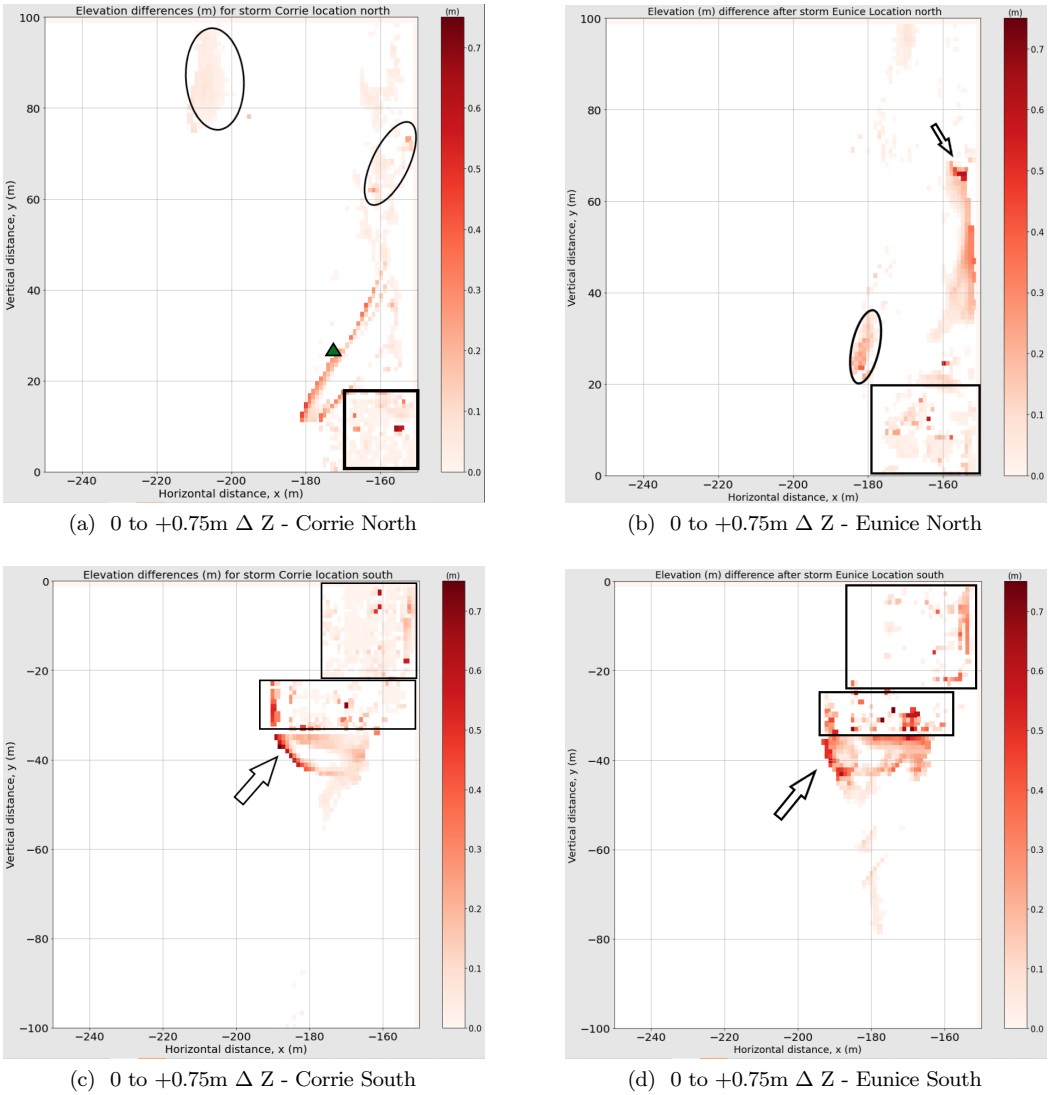

(a) 0 to +0.75m Δ Z - Corrie North

(b) 0 to +0.75m Δ Z - Eunice North

(c) 0 to +0.75m Δ Z - Corrie South

(d) 0 to +0.75m Δ Z - Eunice South

Figure 14: Areas falling under the accretional threshold: an elevation increase up to 0.75m. In the figures, the black squares indicate regions situated in the premise of the beachclub and its terrace. The green triangle indicates the location of tyre tracks in the laser data. The black arrows indicate the location of the embankment, whilst the black ovals indicate other areas of interest

Figure 14 clearly depicts the spatial variation in areas undergoing a positive elevation change ranging from 0 to 0.75m. Due to storm Corrie (Figure 14a), inside the premise of the beachclub (black square), elevation changes up to 0.73m are observed. After quantifying this change , this is found to be a nearly 100 m^2 region of accretion. Moreover, 400 m^2 of the beach experiences accretion in the location of the tyre tracks (green triangle), found 20m north of the beach club. A few other regions are also depicting an accretion in regions close to the waterline, and the foot of the dunes. These regions constitute 37.5% of the areas experiencing an accretion up to 0.75m. For the same region however, storm Eunice (Figure 14b) impacted the beach's northern area differently. In the premise of the beachclub , a smaller area is impacted by this accretion as compared to storm Corrie. Accretion at the location of the tyre track is not observed. Instead, a small 50 m^2 area (black circle) undergoes positive elevation changes of approximately 0.3m. In addition to this, a large area (black arrow) experiences elevation change values of large magnitudes of 0.75m. This is in the location of the foot of the sand dunes, and 60m north of the beach club. Overall, it is observed that a smaller area is impacted by an accretion up to 0.75m for storm Eunice than Corrie. That is merely in terms of area, and not the magnitude of accretion.

In the south of the beach, different features are observed. In the premise of the beach club, positive elevation changes are also observed due to both storms. Storm Corrie (Figure 14c) has also caused positive elevation changes, discrete and scattered in nature. This is an area of approximately 100 m^2. In the location of the embankment (black arrow), a much larger area is impacted. This appears to be a more continuous region, and the location of maximum elevation change. An arc-shaped accretional pattern is depicted in the figure, with greater magnitudes of positive elevation changes 50 m^2 in area. The rest of the embankment covers a greater area, yet comprises of lower elevation gain magnitudes. Comparing the beach's southern location impacted by storm Eunice (Figure 14d), similar areas are impacted , as with storm Corrie. In the premise of the beachclub, nearly the same area amassed accretion up to 0.75m. However, a smaller area is impacted by accretion in the beach's southern location. The region of the embankment (black arrow) is smaller in area , yet depicts higher magnitudes of accretion. Overall, storm Corrie had a 12.5 % larger impact on the beach strip in terms of areas impacted by an accretion up to 0.75m.

The areas affected by a negative elevation difference upto 0.75m are quantified and displayed in Table 7 below.

Table 7: Areas fulfilling threshold 2 ; erosional threshold

Storm name	North area affected (m^2)	South area affected (m^2)	Total area affected (m^2)
Corrie	4409	2788	7197
Eunice	4982	3689	8671

To represent this, Figure 15 shows these regions.

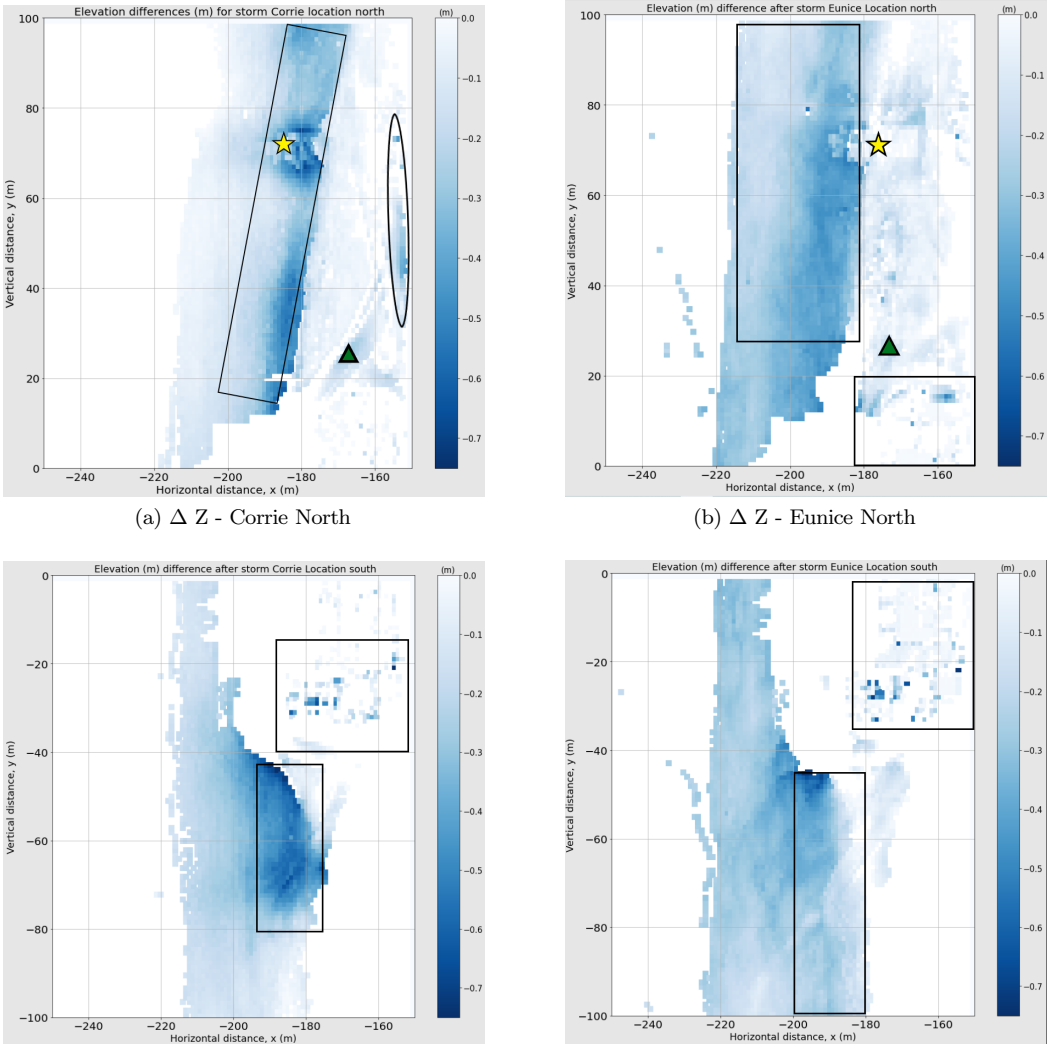

(a) Δ Z - Corrie North

(b) Δ Z - Eunice North

(c) Δ Z - Corrie South

(d) Δ Z - Eunice South

Figure 15: Areas that have undergone elevation losses up to 0.75m. In these figures, a yellow star indicates the location of the concrete tiles, a green triangle depicting the location of the tyre tracks. A black square is used to depict the premise of the beachclub and its terrace. Lastly, black rectangles are used to describe how larger areas have decreased in elevation due to storm Eunice.

Figure 15 displays the areas affected by an height difference up to -0.75m. Just as with accretion, erosional height differences are not only storm dependant, but also vary spatially. Due to storm Corrie (Figure 15a), 4409 m^2 of the beach's northern location experienced height losses up to 0.75m. This is seen in a few locations, such as where tyre tracks are present in the data (green triangle). Moreover, at the foot of the dunes (circled), elevation losses of approximately 0.3m are observed. Much of the erosion that has occurred covers a 20m wide sand strip , indicated by a black

rectangle in the figure. For storm Eunice (Figure 15b), the same is true. Elevation losses reaching 0.75m are observed yet again , however now also at the premise of the beachclub. A smaller area has undergone erosion at the location of the tyre tracks, and less areas have been affected near the foot of the dunes. Erosion is prominent 40m from the waterline, in a region depicted by the black rectangle as well. This is a slightly larger region than with storm Corrie , approximately 40m wide. In the north, nearly 600 m^2 more area was affected by an elevation loss up to 0.75m. In the south, the storms have played a major role in reducing the overall elevation of the beach as well. In the premise of the beachclub and its terrace (black square), scattered and discrete areas have been subjected to a maximum elevation loss of 0.75m. Due to storm Corrie (Figure 15c), a smaller portion of the beachclub experiences these elevation losses, as compared to storm Eunice (Figure 15d). Furthermore, a 20m narrow strip of sand (black rectangle in both subfigures) experiences a maximal elevation loss of 0.75m. Due to storm Corrie, this strip of sand is 800 m^2, yet due to Eunice, this strip is 1100 m^2 in area. In the south overall, more than 900 m^2 area has been subjected to these elevation losses for storm Eunice compared to storm Corrie. Assessing the overall beach strip , it can be concluded that storm Eunice has targeted 20 % more area than storm Corrie in elevation loss up to 0.75m. .

5.4 Changes in sand volume across the beach

The results of the volume change analysis are obtained for the previously mentioned locations A, B, C respectively (see **subsection 4.7**). Table 8 below illustrates the different locations, as well as the volumetric loss of beach material for different grid resolutions. Following this, a summary of the cumulative volumetric losses is provided in Table 9 below.

Table 8: Individual volume changes (ΔV) for areas A, B , C. Resolutions (res) of different magnitudes are tested.

Location	**Storm**	**1m res ΔV (m^3)**	**0.5 m res ΔV (m^3)**	**0.25m res ΔV (m^3)**
A	Corrie	-162.2	-164.7	-91.3
A	Eunice	-207.7	-216.5	-128.5
B	Corrie	-82.8	-90.9	-49.9
B	Eunice	-183.4	-192.7	-104.0
C	Corrie	-270.9	-290.9	-165.8
C	Eunice	-215.7	-227.9	-125.1

Table 9: Summary of Cumulative volumetric changes (ΔV) for locations A, B, C.

Storm name	1m res ΔV (m^3)	0.5 m res ΔV (m^3)	0.25m res ΔV (m^3)
Corrie	-515.9	-546.5	-307.0
Eunice	-606.8	-637.1	-357.6

Volumetric changes quantified prove that for a 900 m^2 area in different locations, the loss of sand occurs in different magnitudes . The sensitivity to resolution change is also accounted whilst determining the volumetric changes of sand. Decreasing the resolution from 1m to 0.5m leads to higher volumetric change estimations. A further reduction of the resolution to 0.25m leads to much lower volumetric changes.After studying these changes, it can be seen that area C experienced a maximum volume loss of sand for both storms, nearly 500 m^3 of sand loss. Area A was impacted to a lesser extent, with a total volume loss of 370 m^3. Lastly, area B seems to be least impacted by volumetric changes, with roughly 270 m^3 of sand displaced after both storms. Overall, there has been a greater change in sand volume in the south compared to the north of the beach. However, with respect to the storms individually, storm Eunice has lead to greater volumetric losses of sand than storm Corrie in the North. In the south however , the opposite is seen to be true and storm Corrie accounts for more sand loss (270 m^3). Overall for the entire beach strip, storm Eunice is seen to be 17% more erosive than storm Corrie with respect to volumetric loss of sand, and targeted 20% more area than storm Corrie.

5.5 Beach profiles

The variations along the north and south beach profiles are displayed in Figure 16 below. The overall variation is highlighted, as well the intermediate changes between the storms.

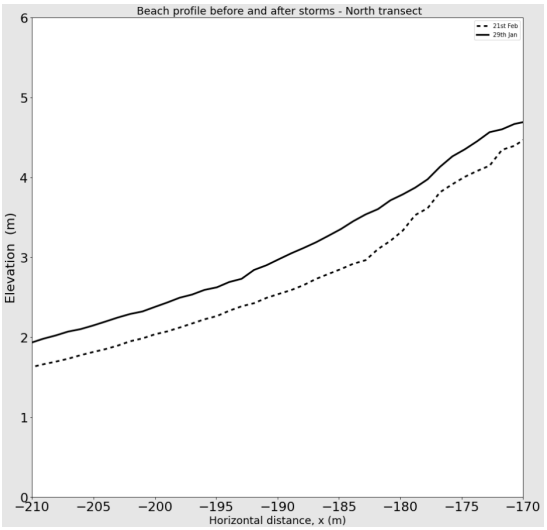

(a) Overall beach profile change between storms - North

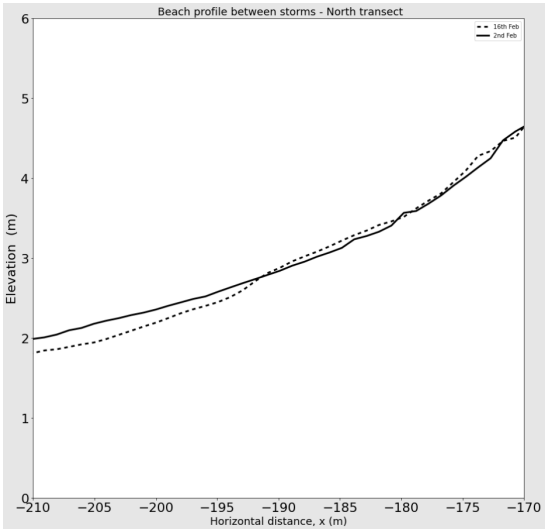

(b) Beach profile before and after both storms - North

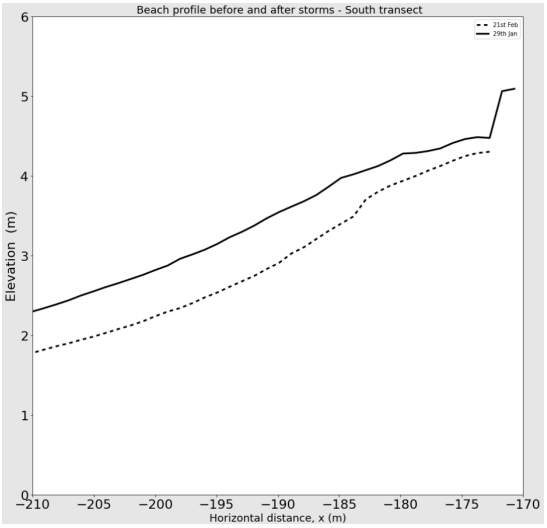

(c) Overall beach profile change between storms - South

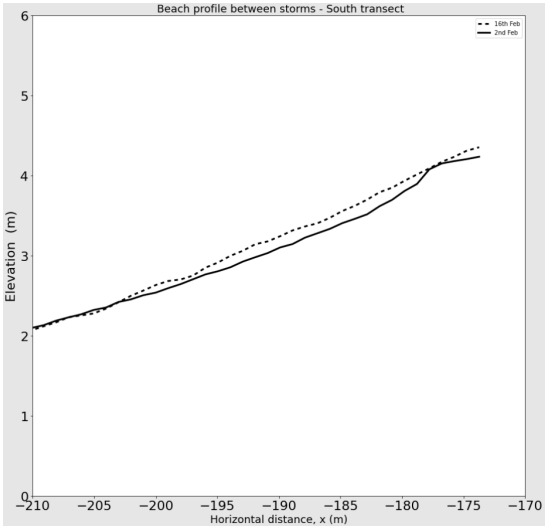

(d) Beach profile before and after both storms- South

Figure 16: Beach profile evolution during storms. Figures 16a/c depict the overall evolution of the beach from the commencement of the first storm to the end of the next storm. On the other hand, Figures 16b/d depict the evolution of the beach profile at the time interval between the two storm. This implies the time after storm Corrie to before storm Eunice.

As shown in the figure, variations occurring in the north and the south are not the same overall for both locations. It is seen that in the north, there is an overall erosion of 0.3m of sand occurring along the north transect. Further away from the waterline, this seems to decrease to 0.1m. In the south of the beach, a similar trend is seen yet is more prominent. Overall, greater elevation differences are observed as compared to the north. The south of the beach experience the same storms differently. Closer to the waterline, the elevation differences are seen to be approximately 0.5m and decline to values as low as 0.15m after the occurrence of both storms. Although understanding overall changes can be advantageous in understanding the impacts of storms, observing variations between one storm and the other provides a lot of information on beach recovery. As shown in Figure 16, the north of beach recovers minimally at horizontal distances of -190m and greater. Closer to the waterline(-210m to -195m), erosion is observed. Thus, this indicates that the maximum range of erosion is 15m away from the waterline by wave action. In the south of the beach, accretion occurs at a horizontal distance of -200 m and greater. The south of the beach experienced accretion after storm Corrie, yet is later impacted by more erosion as storm Eunice commences. It can be seen that approximately 0.2 m of accretion occurs along this transect

5.6 Interpretation of identified changes

To reason the differences in the results, interpretations are made to understand the different behaviours of the storms. Beginning with the elevation difference maps allows for a preliminary understanding of the evolution of the beach elevation as the storms progressed. Close to the waterline in the north's beach location, naturally accreted areas are observed to have occurred after storm Corrie. These are presumably submerged sand bars constituting of sand that has been eroded elsewhere and sedimented underwater. In regions where accretion and erosion occur in the premise of the beach club, chairs, equipment and containers are possibly moved around and lead to spikes in elevation and hence , volumetric changes. These changes are probably anthropogenic and do not provide information on the natural impacts of the storms. Another key location is the foot of the sand dunes. Due to storm Eunice, the beach's northern territory was accreted after the storm yet eroded due to storm Corrie at these locations. Aeolian processes are assumed to contribute to these variations as the dunes are away from the waterline. Closer to the waterline, wave action dominates. As wave action is of higher energy, it can be assumed that in these locations, the beach undergoes erosion more than it does accretion. The location of the concrete tiles are also noted, as all elevation difference maps indicate elevation losses. After visualising and studying the laser data, the concrete tiles appear to be displaced. This displacement could then lead to these elevation losses. Tyre tracks are also studied and are seen to possibly contribute to both accretion and erosion. Depressions in the sand due to the tracks lead to minor elevation losses. A likely reason for this is that sand pushed by the tyres are accreted directly next to these depressions.

In the south of the beach, very few naturally accreted areas are assumed to have occurred. This is because much of the accretion occurring was simply the construction of a protective embankment, as seen in the laser data. Moreover, other areas depicting accretion are yet again situated on the terrace, presumably equipment and chairs as mentioned above. However, the embankment built could have potentially been affected by aeolian processes, yet that is uncertain. Excluding the anthropogenic inputs, the beach still experienced major natural differences due to both storms. To better understand this, wind speeds and directions are studied for both storms by employing a wind rose. This is shown in Figure 17 below.

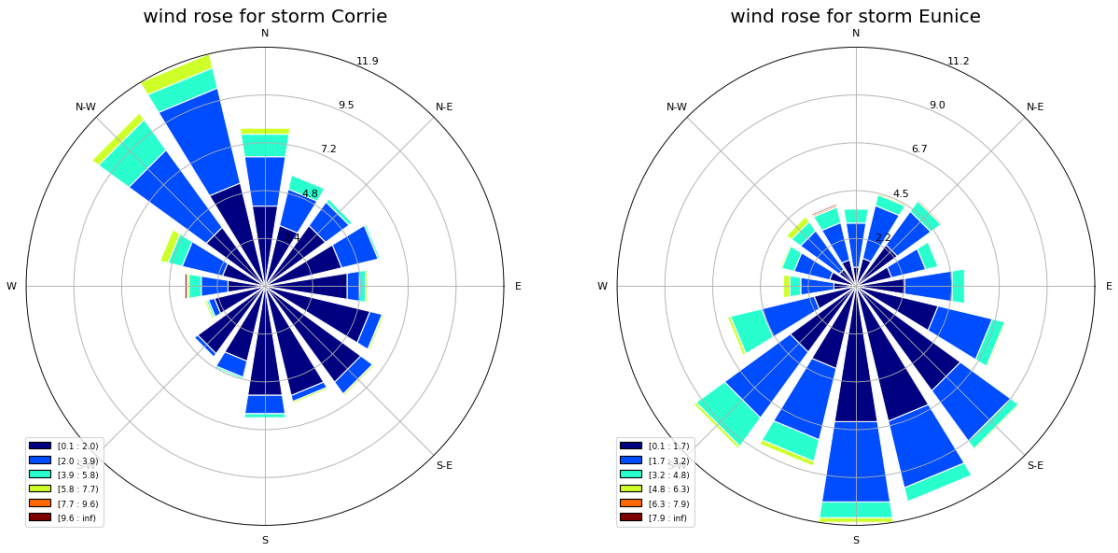

(a) storm Corrie

(b) storm Eunice

Figure 17: Wind speed and direction comparisons of storms Eunice and Corrie.

As seen in the figure, during the occurrence of storm Corrie, strong gusts of wind travelled from the north-northwest and made their way to the beach. Although the wind was blowing from the north, the presence of the beach club could have potentially sheltered the north of the beach by diverting the flow of air. The north therefore still experienced erosion, yet the south of the beach was probably left unprotected. This then lead to greater quantities of sand being removed by aeolian processes and wave action and could explain why the south was impacted greatest. Furthermore, it can be seen that the elevated northerly wind gusts pushed

the wave-fronts southwards. This maybe explains why a great volume of sand was removed in the south and not from the north. In terms of accretion, however, greater accretion is observed to have occurred on the beach due to storm Corrie. This could be due to the artificial embankments being built as a protective measure for the beach club. Accounting for natural accretion, however, sand bars are present in the data in the north of the beach. In terms of wave action, this essentially means that sediments were probably being heavily eroded in the southeast and transported northwest, deposited underwater, leading to the genesis of sandbars.

As per storm Eunice, the dominant wind direction is entirely different. Large wind gusts of over 11.2m/s originate from the south and travel northwards. This also means that the wavefronts travelled in a more northward direction. As this occurs, the wavefronts could have traveled less inland in the south and dissipated energy towards the north. As they dissipate energy, they travel inland and begin to erode the beach. This could explain why storm Eunice lead to greater volumetric losses of sand in the north. Overall, it also seems that as the southerly gusts interacted with the beach club, the diversion of the wind led to large quantities of fine-sand pushed against the structure. This potentially explains why larger accretion values are observed in the results in locations close to the beach club. To reason why storm Eunice is said to have had the greatest impact, is because, in the north of the beach, storm Eunice lead to the greatest volumetric losses although in the south storm Corrie is seen to be more erosive. As storm Eunice eroded a greater area in the north and south, this leads to an overall greater erosive effect on the beach. A possible reason for its erosive effect could be that as the wind direction originates from the south, the erosion occurs along the direction of the beach strip. Moreover, the average wind speed value appears to be slightly higher for storm Eunice than Corrie. The latter also contributes to major differences in the results.

5.7 Impact summary

Table 10: Summarising which storm impacted the beach more based on various locations.

Impact	**North**	**South**	**Overall**	**A**	**B**	**C**
Greater overall elevation loss	Eunice	Corrie	-	-	-	-
Greater average elevation loss	Eunice	Corrie	-	-	-	-
Greatest spread in elevation difference	Equal	Eunice	-	-	-	-
Total area effected by erosion	Eunice	Eunice	Eunice	-	-	-
Total area effected by accretion	Corrie	Corrie	Corrie	-	-	-
Greatest volumetric loss of sand (erosion) 1 m res	Eunice	Corrie	Eunice	Eunice	Eunice	Corrie
Greatest decline in beach profile	Eunice	Corrie	Eunice	Eunice	Eunice	Corrie

Table 11: Summarising the effects on the North and South of the beach. As shown in the table, the beach's south location experiences greater erosive effects than the north.

Impact	**North**	**South**
Greater overall elevation loss (erosion)		✓
Greater average elevation loss		✓
Greatest spread in elevation difference		✓
Total area effected by erosion	✓	
Total area effected by accretion	✓	
Greatest volumetric loss of sand (erosion) 1 m resolution		✓
Greatest decline in beach profile		✓
Greater recovery observed close to waterline	✓	
Greater recovery observed away from waterline		✓

To answer the research question, " **Which of the two storms, Eunice or Corrie, had a greater impact on the beach in Noordwijk?**", this heavily depends on what impact parameter is in question. Overall, storm Eunice has impacted the beach 17 % more than storm Corrie in volume loss, and 20 % in terms of areas impacted by erosion up to 0.75m. Based off of the nine impact parameters displayed in in Table 10, it is evident that storm Eunice has lead to greater erosive effects. In terms of accretion however, storm Corrie dominates assuming due to the creation of the embankment. The north and south of the beach have been impacted differently, the south experiencing overall more averse effects. In this region, greater elevation and volumetric losses of sand are observed.

5.8 Discussion

5.8.1 Uncertainties in reasoning the changes caused by the storms

Although great efforts are made to better understand what could have lead to the formation of accreted and eroded areas, uncertainty is still present. The presence of the embankment is quite clear in the laser data yet this is still an assumption as no beach footage or validation data is present to prove this. Also, the movement of equipment and chairs is not known to be a fact. As per the presumed natural features such as the sand bar, this is yet again another assumption. There could have been an interaction of wave action and aeolian processes , but where this boundary occurs between the two is unknown. Moreover, much of the interpretation is motivated by the weather data which is provided by a weather station 5km away from the beach. This could mean that the situation in the beach is different although highly unlikely.

5.8.2 The use of only four datasets

The research is carried out using four data sets; 2 of which are acquired before each storm, and 2 acquired after. These datasets are consistently used in the research, disregarding datasets that could potentially provide information during the storms. Datasets in between the storms are disregarded, although could be critical in understanding whether the beach experiences recovery between storms, or continues to erode.

5.8.3 The presence of data gaps : shadow effects and water

Although the initial datasets comprised millions of point clouds, data gaps were consistently present. This occurred in regions experiencing "shadow effects" by which objects such as the beachclub and sand dunes cast a shadow on the laser data as the laser does not pass through the objects. These shadows are usually not a major inconvenience if they are small in area, however the shadow caused by the beachclub covers a significantly large portion of the beach data. Had there been no shadow, much more information could have been derived regarding what changes occurred, in addition to why they took place. Furthermore, as laser data is refracted by water, little information can be derived on the transportation of submerged sediments. It is assumed that much of the eroded material has been sedimented underwater, yet that is uncertain. Even studying low tide data is insufficient as after the storms, much of the wave fronts covered a significant portion of the beach. If later datasets are acquired however, beach recovery could have already commenced and the data would be a misrepresentation of what occurred due to the storms.

5.8.4 Division of the beach into northern and southern territories

Throughout this research, the beach has been divided into a northern and southern location to account for the presence of the beachclub. The division was also done to obtain the grids of 1m resolution. The divide between the north and south occurs at the midpoint of the beachclub. Therefore the words north and south are not to be taken too literally and are merely upper and lower halves of the beach data.

5.8.5 Alignment errors and choosing the right grid size

The dataset has been studied for alignment. To verify this, elevation difference histograms were generated and a large peak was noticed to occur for an elevation difference of 0m. This is caused by the presence of the beach club and artificial structures that do not undergo any elevation differences. This then allows for the verification that alignment was successful. This isn't sufficient however and a secondary source of alignment verification must be done such as using a nearby helipad as a reference and looking for elevation changes. If no elevation change is observed then it can be understood that the internal alignment method initially carried out was sufficient.
However, sudden abrupt elevation differences seem to occur even on correctly aligned datasets, in areas where artificial structures are present. A likely reason for this could be a the discrete nature of the gridding process. This process is heavily dependant on the chosen resolution. As the grids are generated using

the median elevation value for a known pixel, if a larger resolution is used more data points can be considered . This essentially means that in an area where a roof is present adjacent to the ground, within the same pixel, the grid assumes that only roof is present if the median elevation value is a roof point. This can be quite confusing, yet using smaller resolutions can eliminate this issue. A downside of using smaller resolution grids however is that in areas further in range from the scanner, less data points are available for processing. If the grid size used is too small, far too little points are considered, oftentimes none and this then leads to large data gaps. The latter makes it data processing tumultuous and overall inaccurate.

5.8.6 Lack of validation data

During the events of the storms, only laser data available from the laser scanner contains sufficient information on the spatial geometry of millions of points on the beach strip. There is no validation available , making it difficult to validate the results obtained. Satellite data can be used , yet their spatial and temporal resolutions deemed unfit. Moreover, extremely poor weather conditions and low hanging clouds lead to poor images. The change detection methodology enlisted is thorough and assumed to be sufficient yet further data processing can always be carried out.

6 Conclusions and Recommendations

6.1 Recommendations

To better understand the in-situ state of the beach and what could have potentially occurred, a few recommendations are listed. When carried out, the following can be advantageous in further refining the research and comparing the impacts of both storms.

Improving the interpretation of identified changes on the beach :

- Study weather data from another proximate weather station and compare for similarities.
- As for the features present on the beach such as the embankment, contact the beachclub to potentially learn about the anthropogenic changes that could have occurred on the beach during the storms.
- Study existing literature of the beach to understand the development of submarine sandbars on dutch beaches such as Noordwijk due to storms.

Dataset acquisition and processing

- Attempt to separate storms Eunice and Dudley weather data. This means that the after storm Eunice dataset must be acquired sooner than the 22nd of February.
- To know whether a grid size is underestimating or over estimating volume changes, determine root mean square errors by setting a particular resolution as a control. The optimum grid size would then be one of lowest error.
- Attempt to acquire data from different parts of the Netherlands, and compare the effects of the storms on different geographic locations.

Data set modification

- Carry out different interpolation methods, such as a linear or cubic interpolation on data gaps. After doing so, compare the results of different interpolation methods. Choosing the best interpolation method can be done by assessing the quality of the sampling points as well as their corresponding distribution. Moreover, an in depth knowledge of the beach's features and the effects of different interpolation methods on these surfaces must be carried out.

6.2 Answering the research questions

The occurrence of storms Eunice and Corrie have resulted in different impacts on the beach of Noordwijk. These impacts are a culmination of the different strengths of the storms, but also the varying locations along the beach strip analysed. This research aimed to answer the following question:

"Which of the two storms, Eunice or Corrie, had a greater impact on the beach in Noordwijk?"
After intensive data processing and careful analysis of the results, it appears that storm Eunice has had a larger impact on the study area, by a value of 17 % in terms of volumetric loss of sand. This is merely a summarised value, however upon closer inspection , the impacts are studied for different parameters. The results show that storm Eunice has lead to more widespread erosion than storm Corrie . This is true for both north and south of the beach. After studying wind rose data, it can be seen that storm Eunice accompanied greater magnitudes of wind speeds , in combination with the southerly winds covering the entire beach strip effectively. Storm Eunice has lead to a greater overall and mean elevation loss values of 0.155m, and eroded 20 % more of the beach area than storm Corrie.

To answer the main research question , the following sub research questions are also answered below :

"When did the storms happen and how can weather data be used to determine the start and end of a storm?"

Storm Corrie commenced on the 29th of January 2022, and ended on the 2nd of February 2022. As per storm Eunice, the storm started on the 16th of January and finished on the 21st of February 2022. To answer this question, weather data of the following types were studied: wind speed, tidal variation, wind

direction, precipitation intensity. To determine suitable start and end points of the storms , it was recognised that these are merely windows of time and not exact temporal moments . By recognising that low tides and low precipitation intensity mean that scans are most visible, these were chosen to be a primary criteria for extracting the right dataset. The start of the storm was chosen by setting a wind speed threshold of 4 m/s and recognising that wind speed values exceeding this imply the start of a storm. When this value is crossed again and continues to show an overall decrease wind speed trend, then the storm has ended. This is only true provided that other factors such as precipitation intensity and wave action are in agreement with this.

"How can changes occurring on the beach profile be quantified?"

Through this study, it is recognised that many remote sensing methods are used to quantify changes along coastlines. This research focuses on the use of a permanent laser scanner obtaining spatial coordinates in X,Y,Z directions. To detect storm-induced changes along the beach, multiple methods are carried out. Initially, a grid is generated to be able to carry out comparisons on pixel pairs. Difference maps can also be used to quantify changes as elevation difference maps clearly indicate where how much change occurs. Moreover, statistical analyses can be done by generating histograms and studying the distributions of data. By doing so, the mean and standard deviation of the spread already provide a preliminary analysis of the elevation differences expected. Area and volumetric change estimations can also be used to quantify changes by determining the total area experiencing erosion and accretion by determining the number of pixels falling under an erosional and accretional threshold . Conversely, if volumetric estimations are used, then by knowing a pixel area and the elevation difference, volumetric changes can be calculated for every pixel and summed to find an overall change. Lastly, transects can be chosen and topographic cross sections can be used to observe the evolution of the beach profile before , in between and after the storms. Studying what occurs in between the storms can be advantageous in understanding whether the beach recovers or simply continues to be eroded between the storms.

"Where do the greatest changes occur along the beach and are there reasons for this change?"

After studying the volumetric changes, it can be seen that a 900 m^2 area in the south experiences 500 m^3 of erosion, whilst for the same area in the north, roughly 270 to 370 m^3 of erosion is observed.
The areas targeted by both storms is also analysed and interpreted for north and south of the beach. Upon doing so, the greatest changes are observed in the south of the beach, 20 m south of the beach club. Upon studying transects, up to an overall 0.5m of sand is seen to be eroded in the south as compared to the north which doesn't exceed an erosion value of 0.3m. A probable reasoning for these changes includes the possible protection of the north by the beach club during the events of the storm by diverting airflow. The south of the beach was more exposed to elevated wind speeds and was a source of sediments for the northwesterly winds occurring during storm Corrie. As for storm Eunice, greater erosive effects were occurring in the north. This was hypothesized to be due to southerly wavefronts migrating northwards and losing energy, hence migrating inland and eroding the north.

References

[1] V. Biase, M. Kuschnerus, and R. Lindenbergh. Permanent laser scanner and synthetic aperture radar data: Correlation characterisation at a sandy beach. *Sensors*, 22:2311, 03 2022. doi: 10.3390/s22062311.

[2] V. D. Biase, M. Kuschnerus, and R. C. Lindenbergh. Permanent laser scanner and synthetic aperture radar data: Correlation characterisation at a sandy beach. *Sensors*, 22, 2022. ISSN 14248220. doi: 10.3390/s22062311.

[3] M. Bitenc, R. Lindenbergh, K. Khoshelham, and P. Waarden. Evaluation of a lidar land-based mobile mapping system for monitoring sandy coasts. *Remote Sensing*, 3:1472–1491, 12 2011. doi: 10.3390/rs3071472.

[4] M. Daneshmand, A. Helmi, E. Avots, F. Noroozi, F. Alisinanoglu, H. S. Arslan, J. Gorbova, R. E. Haamer, C. Ozcinar, and G. Anbarjafari. 3d scanning: A comprehensive survey. *CoRR*, abs/1801.08863, 2018. URL http://arxiv.org/abs/1801.08863.

[5] L. Del Río and F. Gracia. Error determination in the photogrammetric assessment of shoreline changes. *Natural Hazards*, 65, 01 2013. doi: 10.1007/s11069-012-0407-y.

[6] I. Fairley, T. Thomas, M. Phillips, and D. Reeve. *Terrestrial Laser Scanner Techniques for Enhancement in Understanding of Coastal Environments*, pages 273–289. 03 2016. ISBN 978-3-319-25121-9. doi: 10.1007/978-3-319-25121-9_11.

[7] I. Livingstone, G. F. Wiggs, and C. M. Weaver. Geomorphology of desert sand dunes: A review of recent progress. *Earth-Science Reviews*, 80(3):239–257, 2007. ISSN 0012-8252. doi: https://doi.org/10.1016/j.earscirev.2006.09.004. URL https://www.sciencedirect.com/science/article/pii/S0012825206001449.

[8] U. Nations. Factsheet: People and oceans. the ocean conference united nations. *2017*, 2017.

[9] G. Nichols. Sedimentology and stratigraphy gary nichols., 2009.

[10] N. Pfeifer and C. Briese. Laser scanning – principles and applications. 2014. doi: 10.3997/2214-4609.201403279.

[11] T. Planès, J. B. Rittgers, M. A. Mooney, W. Kanning, and D. Draganov. Monitoring the tidal response of a sea levee with ambient seismic noise. *Journal of Applied Geophysics*, 138, 2017. ISSN 09269851. doi: 10.1016/j.jappgeo.2017.01.025.

[12] D. Quincey, M. Bishop, A. Kääb, E. Berthier, B. Flach, T. Bolch, M. Buchroithner, U. Kamp, S. J. Khalsa, T. Toutin, U. Haritashya, A. Racoviteanu, and B. Raup. *Digital terrain modeling and glacier topographic characterization*. 01 2014. doi: 10.5167/uzh-102077.

[13] A. Stanica and G. Ungureanu. Understanding coastal morphology and sedimentology. *Terre et environnement*, 88, 01 2010.

[14] M. Starek. *PROBABILISTIC METHODS FOR IMPROVED CHANGE DETECTION AND PREDICTION ON SANDY BEACHES USING HIGH RESOLUTION AIRBORNE LIDAR*. PhD thesis, 12 2008.

[15] C. van Ijzendoorn, S. Vries, C. Hallin, and P. Hesp. Sea level rise outpaced by vertical dune toe translation on prograding coasts. *Scientific Reports*, 11, 06 2021. doi: 10.1038/s41598-021-92150-x.

[16] S. Vos, K. Anders, M. Kuschnerus, R. Lindenbergh, B. Höfle, S. Aarninkhof, and S. Vries. A high-resolution 4d terrestrial laser scan dataset of the kijkduin beach-dune system, the netherlands. *Scientific Data*, 9: 191, 04 2022. doi: 10.1038/s41597-022-01291-9.

[17] X. Yuan. *Geometric Processing Models For Remotely Sensed Imagery And Their Accuracy Assessment*, pages 105–139. 09 2009. ISBN 978-1-4419-0049-4. doi: 10.1007/978-1-4419-0050-0_5.

Appendices

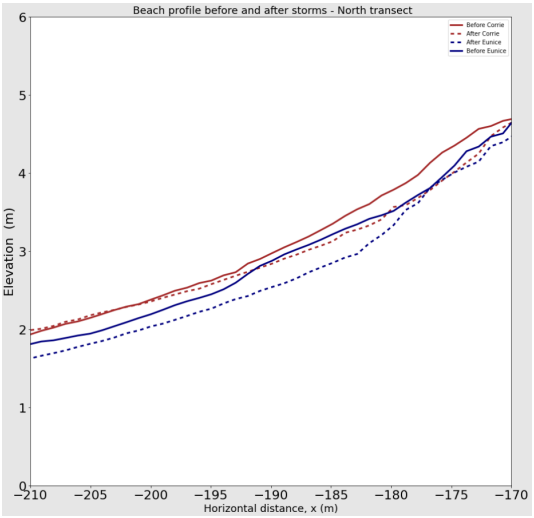

(a) storm Corrie

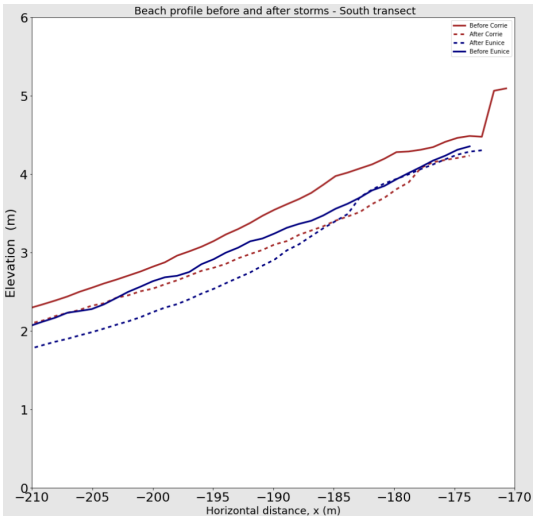

(b) storm Eunice

Figure 18: Temporal evolution of beach profile

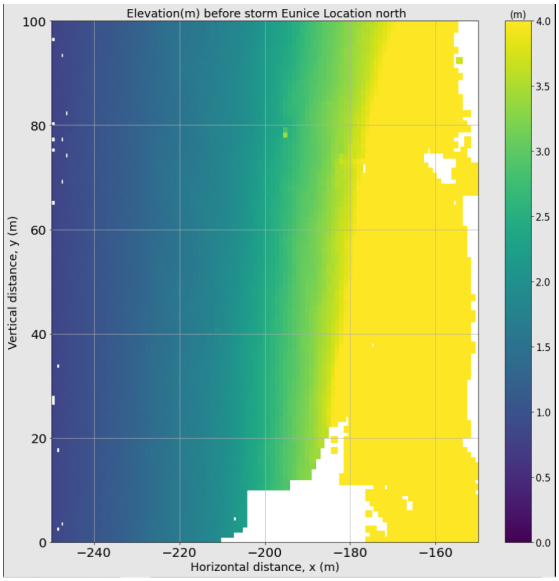

(a) Before Eunice North

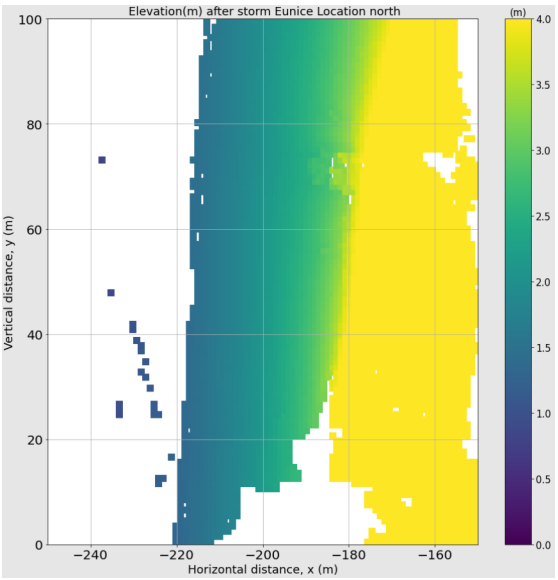

(b) After Eunice North

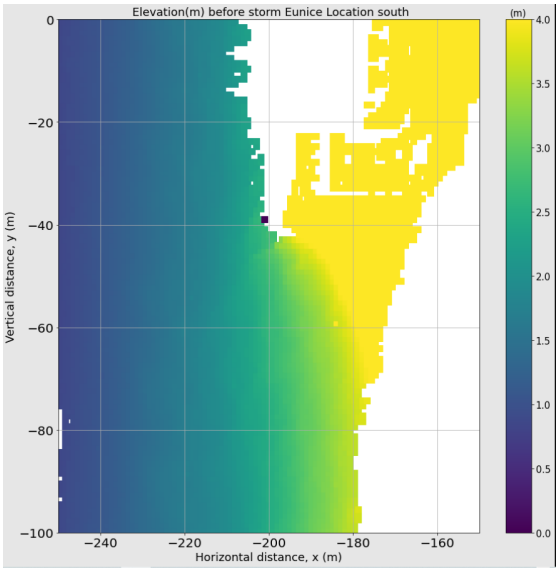

(c) Before Eunice South

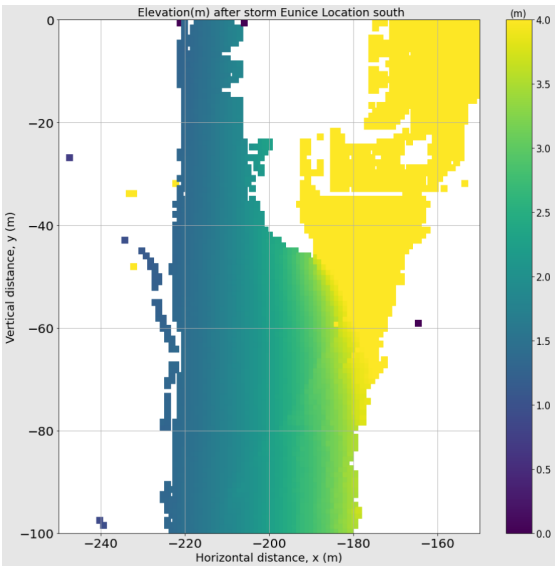

(d) After Eunie South

Figure 19: Elevation maps for storm Eunice

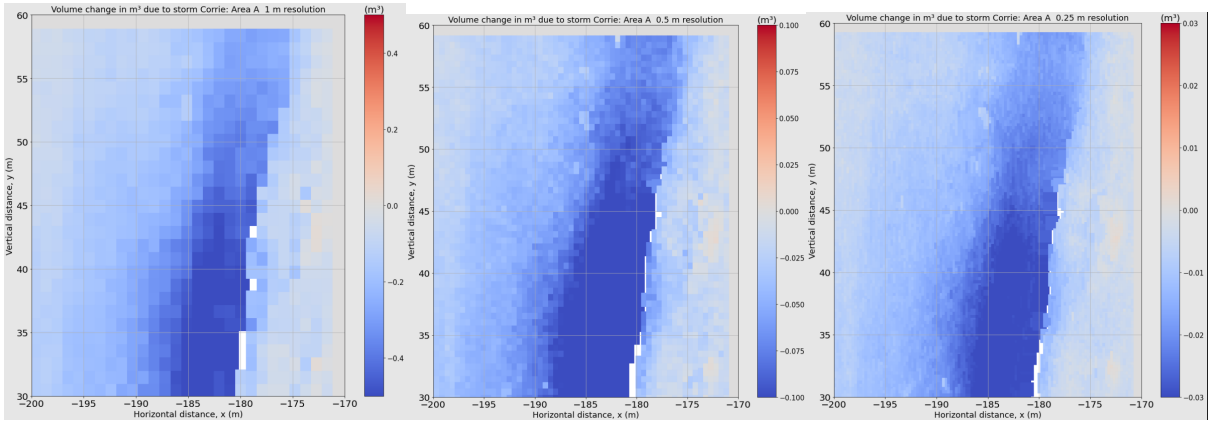

(a) 1m resolution - Corrie (b) 0.5m resolution - Corrie (c) 0.25m resolution- Corrie

(d) 1m resolution- Eunice (e) 0.5m resolution- Eunice (f) 0.25m resolution- Eunice

Figure 20: Storm induced volumetric changes for different resolutions- area A

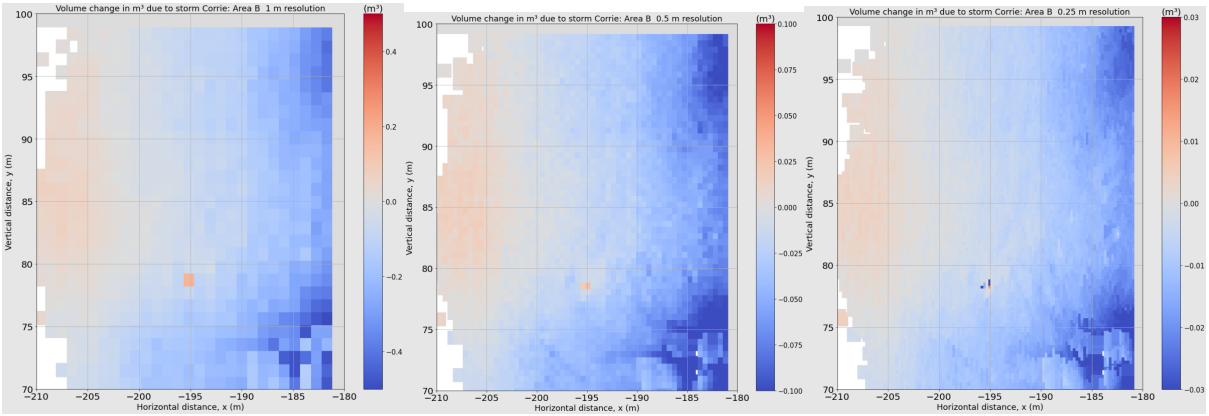

(a) 1m resolution - Corrie (b) 0.5m resolution - Corrie (c) 0.25m resolution- Corrie

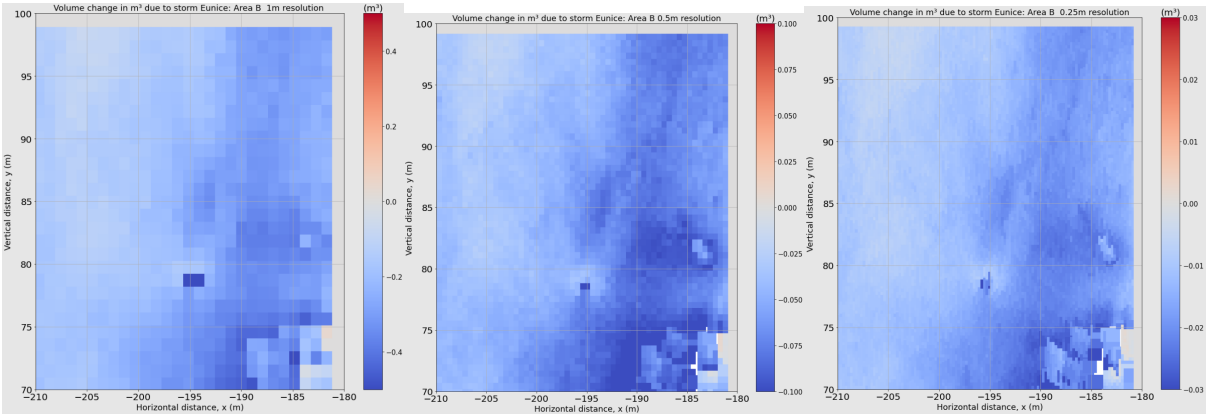

(d) 1m resolution- Eunice (e) 0.5m resolution- Eunice (f) 0.25m resolution- Eunice

Figure 21: Storm induced volumetric changes for different resolutions- area B

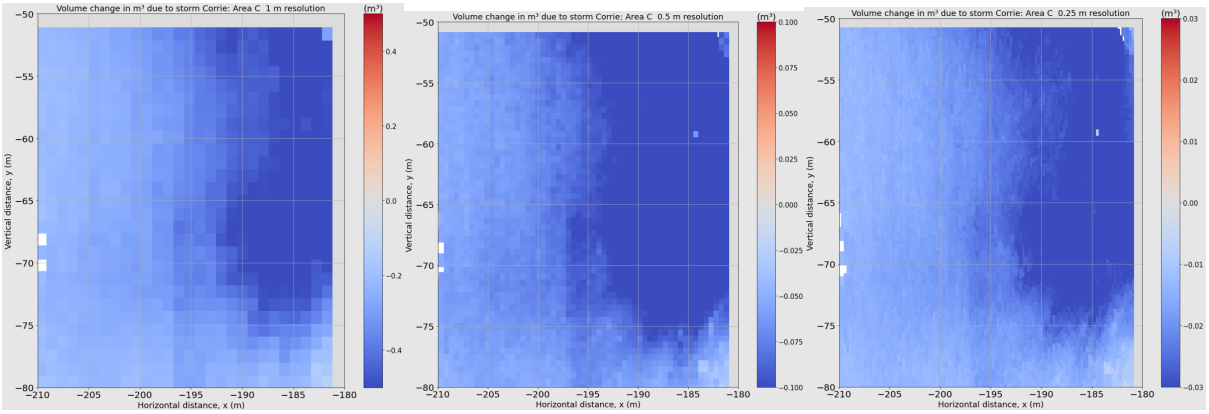

(a) 1m resolution - Corrie (b) 0.5m resolution - Corrie (c) 0.25m resolution- Corrie

(d) 1m resolution- Eunice (e) 0.5m resolution- Eunice (f) 0.25m resolution- Eunice

Figure 22: Storm induced volumetric changes for different resolutions- area C

```
# coding: utf-8

# In[ ]:


import pandas as pd
import numpy as np
import matplotlib.pyplot as plt

from os import  listdir,path
import laspy

def read_file(filename, read_refl=False):

    z_scanner = 55.755 # scanner elevation in m
    max_elev = 20 # relative to the ground
    min_elev=-20# max z value needed in data in m
    max_x = -150 # max x-coordinate to filter out points on hotel terrace

    if '.asc' in filename:

        data = pd.read_csv(filename, delim_whitespace=True ,sep = ',' ,
                           header = 1)

        if not 'x' in data.columns:
            data = pd.read_csv(filename, delim_whitespace=True)
            data.columns = ['x', 'y', 'z', 'ref']

        if read_refl == False:
            data = data.iloc[:,:3]

    elif '.laz' in filename:

        inFile = laspy.read(filename) #laspy.read(filename)

        data = pd.DataFrame({'x' : np.array(inFile.x), 'y' : np.array(inFile.y),
                             'z' :np.array(inFile.z)})

        if read_refl:
            reflectance = inFile.points["point"]["reflectance"] *
            inFile.header.vlrs[0].reflectance.scale[0]
            data['ref'] = reflectance

    else:
        raise ValueError('unknown file format:'+filename)

# apply filter on z- and x-coordinate
# if needed add filter on y-coordinate here
# make sure
    data=data[min_elev-z_scanner<=data.z] # min elevation is a negative number,
#z scanner is a positibe number, now we want the z values from the scanner to
#be not as negative as the most negative number
    data = data[data.z<=max_elev-z_scanner] # make sure the z that you have

    data= data[data.x<=max_x] # make sure that its not taking the hotel
#X cordinates
```

```
    if not 'aligned' in filename:
# rotate data to correct for inclination:
        display(data1)
        inc_file = filename[:-4]+'_incl.asc'
        if path.isfile(inc_file):
            temp_data = pd.read_csv(inc_file, delim_whitespace=True, header = None)
            roll  = np.round(temp_data.iloc[:,0].mean(),4)
            pitch = np.round(temp_data.iloc[:,1].mean(),4)

            roll = -roll * np.pi/180.0
            pitch = - pitch *np.pi/180.0
            trafo_matrix = np.asarray([[np.cos(pitch), 0, np.sin(pitch)],

                [np.sin(pitch)*np.sin(roll), np.cos(roll),
                -np.cos(pitch)*np.sin(roll)],[-np.sin(pitch)*np.cos(roll),
                np.sin(roll), np.cos(pitch)*np.cos(roll)]])

            rotation = lambda inp: np.dot(np.asarray(inp), trafo_matrix)
            data[['x', 'y','z']] = data[['x', 'y','z']].apply(rotation, axis=1,
                                                    result_type='expand')
        else:
            print('Rotation file not found!')
        display(data)
# correct for scanner height, so that z-coordinate corresponds to NAP and is not negati
    data1.z = data1.z+z_scanner


    print(str(len(data1))+' data points have been extracted from '+filename)

    return data1


#change resolution accordingly

data1x=data1.x.tolist()
data1x = np.array(data1x)

data1y=data1.y.tolist()
data1y = np.array((data1y))


data1z = data1.z.tolist()
data1z = np.array(data1z)


nx = 100
ny = 100

x = np.linspace(-250, -150, nx)
y = np.linspace(0, 100, ny)


xbox = np.zeros ((nx-1,ny-1))
ybox = np.zeros ((nx-1,ny-1))
zbox1 = np.zeros ((nx-1,ny-1))
```

```
for i in range(nx-1):
    for j in range(ny-1):
        if  data1x[data1x>x[i]].any() and  data1x[data1x< x[i+1]].any():
            if data1y[data1y>y[j]].any() and  data1y[data1y< y[j+1]].any():
                xbox[i,j] = (x[i]+x[i+1])/2
                ybox[i,j] = (y[j]+y[j+1])/2
#zbox_list = data1.z[x[i] <data1.x< x[i+1] and y[j]<data1.y< y[j+1]]
                zbox_list = data1[(x[i] < data1x) & (data1x < x[i+1]) & (y[j]< data1y)
                                  & (data1y< y[j+1])].z.values
                zbox1[i,j] = np.median(zbox_list)

        else:
            print('no')
#print (xbox[i,j])


# Generate difference map


Z_diff = np.zeros((nx-1,ny-1))
for i in range(len(zbox1)-1):
    for j in range(len(zbox1)-1):
        Z_diff[i,j] =zbox2[i,j]-zbox1[i,j]

# Generate volumetric differences

Z_volume1 = np.zeros((nx-1,ny-1))
for i in range(len(zbox1)-1): #1m resolution
    for j in range(len(zbox1)-1):
        Z_volume1[i,j] =Z_diff[i,j]*1


Z_volume1 = np.zeros((nx-1,ny-1))
for i in range(len(zbox1)-1):
    for j in range(len(zbox1)-1):
        Z_volume1[i,j] =Z_diff[i,j]*0.5**2 # 0.5m resolution

Z_volume1 = np.zeros((nx-1,ny-1))
for i in range(len(zbox1)-1):
    for j in range(len(zbox1)-1):
        Z_volume1[i,j] =Z_diff[i,j]*0.25**2 # 0.25m resolution


# Area estimations

z4=np.ndarray.flatten(zdiff4_1m).tolist()
df4=pd.DataFrame({'x':x,'y':y,'z':z4})
df4_filtered1=df4[(df4.z > 0) & (df4.z < 0.75)]
df4_filtered2=df4[(df4.z > -0.75) & (df4.z <0)]
print(df4_filtered1.shape)
print(df4_filtered2.shape)

# PLOTS



import matplotlib.patches as mpatches
# rect1=mpatches.Rectangle((-200,30),30,0,
```

```
# fill = False,
# color = "red",
# linewidth = 2)
rect2=mpatches.Rectangle((-220,-60),48,0,
                         fill = False,
                         color = "red",
                         linewidth = 3)
rect3=mpatches.Rectangle((-215,80),60,0,
                         fill = False,
                         color = "red",
                         linewidth = 3)


plt.figure(figsize=(15,15))
scat = plt.scatter(data4.x, data4.y, c=data4.z, s=1)
plt.xlim([-250,-150])
plt.ylim([-100,100])
plt.clim(-1,5)
cbar=plt.colorbar(scat)
tick_font_size = 15
cbar.ax.tick_params(labelsize=tick_font_size)
cbar.ax.set_title('(m)', fontsize=15)
plt.tick_params(axis='x', labelsize=16)
plt.tick_params(axis='y', labelsize=16)

plt.title('␣Elevation(m)␣after␣storm␣Eunice', fontsize=20)
plt.xlabel('Horizontal␣distance,␣x␣(m)',fontsize=18)
plt.ylabel('Vertical␣distance,␣y␣(m)',fontsize=18)
# plt.gca().add_patch(rect1)
plt.gca().add_patch(rect2)
plt.gca().add_patch(rect3)
plt.text(-215, -55,'South␣transect',fontsize=20, color="black", weight="bold")
plt.text(-205, 85,'North␣transect',fontsize=20, color="black", weight="bold")

# Generating transects


x=np.ndarray.flatten(xbox).tolist()
y=np.ndarray.flatten(ybox).tolist()
z1=np.ndarray.flatten(zbox1).tolist()
z2=np.ndarray.flatten(zbox2).tolist()
z3=np.ndarray.flatten(zbox3).tolist()
z4=np.ndarray.flatten(zbox4).tolist()

n1=pd.DataFrame({'x':x,'y':y,'z':z1})
n1=n1.dropna()

n1=n1[(n1.y <80.5) & (n1.y > 80)]



n2=pd.DataFrame({'x':x,'y':y,'z':z2})
n2=n2.dropna()
n2=n2[(n2.y <80.5) & (n2.y > 80)]



n3=pd.DataFrame({'x':x,'y':y,'z':z3})
```

```
n3=n3.dropna()
n3=n3[(n3.y <80.5) & (n3.y > 80)]



n4=pd.DataFrame({'x':x,'y':y,'z':z4})
n4=n4.dropna()
n4=n4[(n4.y <80.5) & (n4.y > 80)]



plt.figure(figsize=(15,15))
fig, ax = plt.subplots(figsize=(15, 15))
plt.title('Beach profile before and after storms - North transect', fontsize=18)
sns.lineplot(data=n1, x='x', y='z', label='Before Corrie', ax=ax, color='brown', lw=3)
sns.lineplot(data=n2, x='x', y='z', label='After Corrie', ax=ax, color='brown',
             style=True, dashes=[(2,2)], legend=False , lw=3)
sns.lineplot(data=n4, x='x', y='z', label='After Eunice', ax=ax ,color='navy',
             style=True, dashes=[(2,2)], legend=False, lw=3)
sns.lineplot(data=n3, x='x', y='z', label='Before Eunice', ax=ax, color='navy', lw=3)
plt.xlabel('Horizontal distance , x (m)',fontsize=18)
plt.ylabel('Elevation  (m)',fontsize=22)
plt.tick_params(axis='x', labelsize=22)
plt.tick_params(axis='y', labelsize=22)
plt.xlim(-210,-170)
plt.ylim(0,6)
fig.show()


# weather data


#Noordwijkerhout , station ID :Station ID: 160570f6-47c1-ea11-bf21-0003ff5982ee ,
#Cordinates : 52.2541,4.4894


#windspeed in m/s


df_11 = pd.read_csv('windspeed_corrie.csv') #importing data

new_df_wc=df_11[df_11['windspeed'].str.contains("-") == False]
# dropping the Nan Values
fig1= px.line(new_df_wc,x=new_df_wc['datum'], y=new_df_wc['windspeed'])
fig1.update_layout(autotypenumbers='convert types')
fig1.update_traces(line_color='#d62728')
fig1.update_layout(title="Storm Corrie Wind Speed Time Series",
                   xaxis_title="Date and Time",
                   yaxis_title="windspeed(m/s)",
                   legend_title="Legend Title",
                   font=dict( family="Times New, monospace",
                                        size=12,   color="Black"))
go.Layout(yaxis=dict(range=[0, 10]))
fig1.show()
```

```
# precipitation in mm/hr


df_12= pd.read_csv('precipitation_corrie.csv') #importing data

fig2 = px.line(new_df_wc,x=df_12['datum'], y=df_12['Precipitation'])
#NOTE : I CHECKED FOR NAN VALUES AND DIDN'T FIND ANY
fig2.update_layout(autotypenumbers='convert types')
fig2.update_traces(line_color='#1f77b4')
fig2.update_layout(title="Storm Corrie Precipitation Time Series",
                   xaxis_title="Date and Time",
                   yaxis_title="Precipitation (mm/hr)",
                   legend_title="Legend Title",
                   font=dict( family="Times New, monospace",
                                                          size=12,   color="Black"))
go.Layout(yaxis=dict(range=[0, 10]))
fig2.show()


# Wind direction
from windrose import WindroseAxes
x=df1['direction'].values.tolist()
yy=df1['velocity'].values.tolist()
y=[float(x) for x in yy]
ax = WindroseAxes.from_ax()
ax.bar(x,y, normed=True, opening=0.8, edgecolor='white',cmap=plt.cm.jet)
plt.title(' wind rose for storm Corrie ', fontsize=18)
ax.set_legend()
```